

1-1-1980

# The effect of material variables on the fatigue fracture mechanisms in poly(vinyl chloride) (PVC).

Clare Marie Rimnac

Follow this and additional works at: <http://preserve.lehigh.edu/etd>



Part of the [Materials Science and Engineering Commons](#)

---

## Recommended Citation

Rimnac, Clare Marie, "The effect of material variables on the fatigue fracture mechanisms in poly(vinyl chloride) (PVC)." (1980). *Theses and Dissertations*. Paper 1728.

This Thesis is brought to you for free and open access by Lehigh Preserve. It has been accepted for inclusion in Theses and Dissertations by an authorized administrator of Lehigh Preserve. For more information, please contact [preserve@lehigh.edu](mailto:preserve@lehigh.edu).

THE EFFECT OF MATERIAL VARIABLES  
ON THE FATIGUE FRACTURE MECHANISMS  
IN POLY(VINYL CHLORIDE) (PVC)

by

Clare Marie Rimnac

A Thesis

Presented to the Graduate Committee

of Lehigh University

in Candidacy for the Degree of

Master of Science

in

Metallurgy and Materials Engineering

Lehigh University

1980

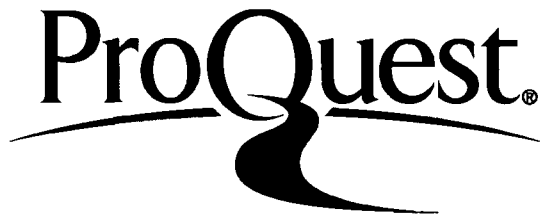
ProQuest Number: EP76000

All rights reserved

INFORMATION TO ALL USERS

The quality of this reproduction is dependent upon the quality of the copy submitted.

In the unlikely event that the author did not send a complete manuscript and there are missing pages, these will be noted. Also, if material had to be removed, a note will indicate the deletion.



ProQuest EP76000

Published by ProQuest LLC (2015). Copyright of the Dissertation is held by the Author.

All rights reserved.

This work is protected against unauthorized copying under Title 17, United States Code  
Microform Edition © ProQuest LLC.

ProQuest LLC.  
789 East Eisenhower Parkway  
P.O. Box 1346  
Ann Arbor, MI 48106 - 1346

Certificate of Approval

This thesis is accepted and approved in partial fulfillment  
of the requirements for the degree of Master of Science.

April 16, 1980  
(date) /

[Richard W. Hertzberg]  
(Professor in Charge)

[Alan W. Pense]  
(Chairman of Department)

### Acknowledgements

For their guidance, patience and support, the author wishes to express her sincere appreciation to her advisors, Dr. R. W. Hertzberg, and Dr. J. A. Manson. The author is indebted to Philip E. Bretz for many enlightening discussions, and especially for his friendship. Many thanks go to Dr. Michael D. Skibo for helpful consultation regarding the current research. The assistance of the technical and secretarial staff, and the machine shop throughout this project is also greatly appreciated.

The author wishes to thank S. M. Webler for the characterization of the poly(vinyl chloride) samples studied in this thesis. The assistance of Dr. E. A. Collins (then of the B. F. Goodrich Co.) and of Dr. Richard K. Chan (Air Products, Inc.) in arranging for molecular weight determinations (Series 1 and 2, and CP, respectively) is gratefully acknowledged.

Finally, the author wishes to thank the Polymer Division of the National Science Foundation for financial support through Grant No. DMR 77-10063.

## Table of Contents

|  | <u>Page</u> |
|--|-------------|
| <u>Title Page</u>                          | i           |
| <u>Certificate of Approval</u>             | ii          |
| <u>Acknowledgements</u>                    | iii         |
| <u>Table of Contents</u>                   | iv          |
| <u>List of Figures</u>                     | vi          |
| <u>List of Tables</u>                      | x           |
| <u>Abstract</u>                            | 1           |
| <u>Introduction</u>                        | 3           |
| <u>Experimental Procedures</u>             | 9           |
| Materials                                  | 9           |
| Characterization                           | 9           |
| Sample Preparation                         | 11          |
| Fatigue Testing                            | 11          |
| Fractographic Examination                  | 13          |
| <u>Experimental Results and Discussion</u> | 14          |
| Fatigue Crack Propagation in PVC           | 14          |
| Molecular Weight Effect                    | 14          |
| Residual Orientation Effect                | 19          |
| Fractographic Analysis of PVC              | 23          |
| Macromorphology                            | 23          |
| Micromorphology                            | 40          |
| PVC Micromorphology at low M               | 49          |
| <u>Conclusions</u>                         | 57          |

|                   |    |
|-------------------|----|
| <u>References</u> | 58 |
| <u>Vita</u>       | 61 |

## List of Figures

| <u>Figure</u> |   | <u>Page</u> |
|---------------|---|-------------|
| 1             | Fatigue crack growth rate $da/dN$ as a function of stress intensity range $\Delta K$ for a number of polymers.  | 5           |
| 2             | Compact tension specimen for generation of fatigue crack propagation data.  | 12          |
| 3             | Effect of molecular weight on fatigue crack propagation of PVC; $R = 0.1$ , 10 Hz (CP $M_w = 1.08 \times 10^5$ ).   | 15          |
| 4             | Effect of molecular weight and orientation on the fatigue crack growth rate of PVC.<br>(● ■ ▲) = $90^\circ$ , (○ □ △) = $0^\circ$ test orientation.   | 16          |
| 5             | Relationship between FCP rate and $1/M$ for PVC ( $\Delta K = 0.7 \text{ MPa}\sqrt{\text{m}}$ ) and PMMA ( $\Delta K = 0.6 \text{ MPa}\sqrt{\text{m}}$ ).<br>(● ■ ▲) = $90^\circ$ , (○ □ △) = $0^\circ$ test orientation. | 17          |
| 6             | Effect of orientation and mean stress on FCP behavior in CP PVC ( $M_w = 1.08 \times 10^5$ ).   | 22          |
| 7             | Discontinuous growth band size as a function of $\Delta K$ for Series 1 PVC.  | 24          |
| 8             | DG band size as a function of $\Delta K$ and test orientation for Series 2 PVC. (a) 132-1; (b) 133-1; (c) 134-1; (d) 135-1.   | 25-28       |
| 9             | DG band size as a function of $\Delta K$ and test orientation for CP PVC. (a) $90^\circ$ , $0^\circ$ ; (b) $+45^\circ$ , $-45^\circ$ .  | 29-30       |



|    |  |    |
|----|--|----|
| 10 | Discontinuous growth band size as a function of $\Delta K$ and test orientation for PVC. No DG bands observed below $M_w = 0.95 \times 10^5$ .   | 31 |
| 11 | Effect of DOP content on DG band sizes of PVC.   | 36 |
| 12 | Effect of molecular weight on cyclic stability ( $N^*$ ) of crazes in PVC as a function of $\Delta K$ and test orientation.  | 37 |
| 13 | Cyclic stability ( $N^*$ ) as a function of molecular weight ( $M_w$ ).  | 39 |
| 14 | Effect of DOP content on cyclic stability ( $N^*$ ) of crazes in PVC as a function of $\Delta K$ .   | 41 |
| 15 | SEM fractograph showing void gradient and stretch zone associated with adjacent DG bands. Arrow indicates direction of crack growth, $M_w = 0.96 \times 10^5$ , 13% DOP, $\Delta K = 0.5 \text{ MPa}\sqrt{\text{m}}$ . | 43 |
| 16 | DG band morphology of low M PVC as a function of stress intensity level. (a) $\Delta K = 0.42 \text{ MPa}\sqrt{\text{m}}$ ; (b) $\Delta K = 0.77 \text{ MPa}\sqrt{\text{m}}$ . $M_w = 0.97 \times 10^5$ .              | 44 |
| 17 | DG band morphology of high M PVC revealing a more ragged structure than at low M. $M_w = 1.69 \times 10^5$ , $\Delta K = 0.66 \text{ MPa}\sqrt{\text{m}}$ .  | 45 |

|    |   |       |
|----|---|-------|
| 18 | Effect of plasticizer on size and structure of DG band morphology at high M. (a) $M_w = 2.1 \times 10^5$ , 0% DOP, $\Delta K = 0.89 \text{ MPa}\sqrt{\text{m}}$ ; (b) $M_w = 2.25 \times 10^5$ , 13% DOP, $K = 0.81 \text{ MPa}\sqrt{\text{m}}$ .   | 46    |
| 19 | Comparison of DG band morphology of an unmodified PVC fracture sample and a CP PVC fracture sample. (a) $M_w = 1.06 \times 10^5$ , $\Delta K = 0.74 \text{ MPa}\sqrt{\text{m}}$ ; (b) $M_w = 1.07 \times 10^5$ , $\Delta K = 0.68 \text{ MPa}\sqrt{\text{m}}$ .   | 48    |
| 20 | Fracture surface of PVC at very low M. (a) Constant sized bands, found at low $\Delta K$ levels ( $\Delta K = 0.4 \text{ MPa}\sqrt{\text{m}}$ ); (b) Striation-like lineage (within crack arrest marks) corresponding to macroscopic growth rate, near fast fracture. $\Delta K = 0.64 \text{ MPa}\sqrt{\text{m}}$ ; (c) High magnification of bands in (b), revealing finer internal lineage. Markers indicate boundaries of each "striation". $M_w = 0.61 - 0.67 \times 10^5$ . | 50-51 |
| 21 | FCP of sample 132-1, showing discontinuity in crack growth rate at $\Delta K \approx 0.8 \text{ MPa}\sqrt{\text{m}}$ associated with fracture mechanism transition. $M_w = 0.95 \times 10^5$ , $0^\circ$ test orientation.  | 53    |
| 22 | (a) Light micrograph of fracture transition of sample 132-1. Light patchy areas indicate roughness of DG bands, while lower contrast  | 55-56 |

region indicates smoother textured.  $\Delta K = 0.8 \text{ MPa}\sqrt{\text{m}}$ ; (b) Periodic array of finer fracture lines comprising each larger band. Marks indicate boundaries of large bands.  $\Delta K = 1.76 \text{ MPa}\sqrt{\text{m}}$ .  $M_w = 0.95 \times 10^5$ .

List of Tables

| <u>Table</u> |   | <u>Page</u> |
|--------------|---|-------------|
| I            | Materials   | 10          |
| II           | Calculated Yield Stresses for<br>CP and Series 1 and 2 Using<br>the Dugdale Model | 33          |

### Abstract

The fatigue crack propagation (FCP) resistance and fracture surface micromorphology of poly(vinyl chloride) (PVC) was studied as a function of molecular weight (M), plasticizer content, and residual orientation. With regard to fatigue crack growth, previous studies of the effect of M on FCP were extended and earlier conclusions were verified. In the range of  $M_w$  between  $6.0 \times 10^4$  and  $2.2 \times 10^5$ , M strongly affected the fatigue crack growth rate  $\left(\frac{da}{dN}\right)$  at a given stress intensity ( $\Delta K$ ) level and followed the relationship  $da/dN = A e^{1/M} \Delta K^n$ . Residual orientation due to processing was found to have a slight, but consistent effect on fatigue behavior, with the greatest FCP resistance occurring when crack growth was perpendicular to the direction of residual chain alignment. The effect of residual orientation on fatigue crack growth was found to be less pronounced at high M.

Regarding fatigue fracture surface micromorphology, particular attention was given as to how the above variables affected the formation of discontinuous growth bands (DGB's). DG bands, which form on a number of polymeric solids under cyclic loading, represent successive increments of crack extension through a craze zone. As expected, DGB width showed little change in size over the molecular weight range of sample orientations examined, and increased in size with increasing plasticizer content. On the other hand, the cyclic stability of these bands increased markedly with increasing molecular weight, but to a lesser extent with additions of a plasticizer. The

internal structure of the bands became more ragged with increasing M, while the addition of a plasticizer re-established the crisp and well-defined micromorphology associated with DG bands in low-M polymers.

## Introduction

With the increasing use of engineering plastics in structural applications, study of the mechanical behavior of these materials has become of practical as well as fundamental interest. To this end, much research has been directed toward the static properties of polymers. In recent years, however, attention also has been given to the response of polymers to cyclic loading. In this regard, fatigue crack propagation (FCP) studies are of particular interest because processed materials nearly always contain imperfections. Under the application of cyclic loads (which may be well below the static yield strength) these flaws can grow and ultimately result in component failure. Thus, when considering the fatigue response of polymeric materials, it is prudent to assume that a flaw already exists. Therefore, a major fraction of a specimen's cyclic life is considered to be spent in the propagation, rather than the initiation of a flaw; this has been shown for the case of poly (vinyl chloride) (PVC) by Hutchinson et al.<sup>(1)</sup> For this reason, linear elastic fracture mechanics concepts have been shown to be very useful in the evaluation of the fatigue crack propagation (FCP) behavior of engineering plastics.<sup>(2-4)</sup>

The response of a precracked solid to an applied stress can be described by the stress intensity factor, which is a measure of the stress amplification at the crack tip and is defined by

$$K = Y \sigma \sqrt{a} \quad (1)$$

where K is the stress intensity factor, Y is a calibration factor

which accounts for specimen geometry,  $\sigma$  is the applied stress and  $a$  is the length of the crack. If the solid experiences cyclic loading, then  $\Delta K$  can be determined, where  $\Delta K$  is calculated using  $\sigma_{\max} - \sigma_{\min}$  ( $\Delta\sigma$ ) in equation (1). This stress intensity factor range has been shown to be related to the fatigue crack growth rate by the following equation<sup>(5)</sup>

$$\frac{da}{dN} = A \Delta K^n \quad (2)$$

where  $\frac{da}{dN}$  is the increment of crack growth per loading cycle,  $\Delta K$  is the stress intensity factor range and  $A$  and  $n$  are constants, dependent upon material and test variables.

Using the relationships given in equations 1 and 2, a large body of FCP data has been generated for a variety of polymeric materials, both amorphous and semi-crystalline. Figure 1 is a composite plot of  $da/dN$  vs  $\Delta K$  which allows one to compare the relative resistance to fatigue crack growth for a number of different polymeric solids. For example, it is seen that amorphous polymers, e.g., poly(methyl methacrylate) (PMMA), polystyrene (PS) and poly(vinyl chloride) (PVC) are in general less resistant to fatigue crack growth than semi-crystalline polymers like nylon, or poly(vinylidene fluoride) (PVF<sub>2</sub>).

Understanding the fatigue crack propagation resistance of a polymer involves not only macroscopic measurement, but also microscopic examination of the fatigue fracture mechanisms involved and their relationship to polymer deformation mechanisms (crazing or shear).<sup>(6-9)</sup> One of the most common morphological features found



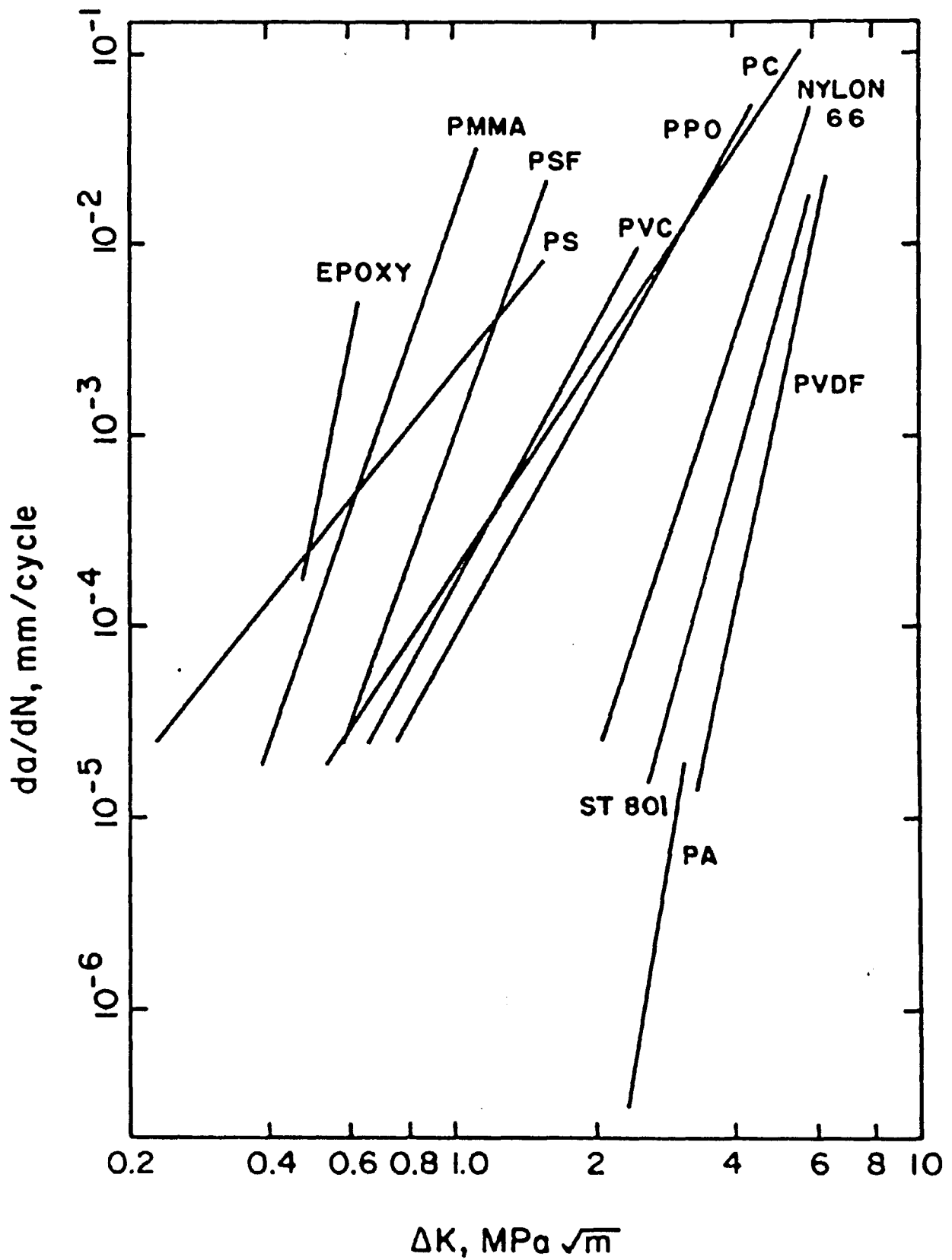


Figure 1. Fatigue crack growth rate  $da/dN$  as a function of stress intensity range  $\Delta K$  for a number of polymers.

in the fatigue fracture of many polymeric solids, as well as metal alloys, is the fatigue striation. Such markings, which represent the successive positions of the crack front at the end of each loading cycle, are oriented normal to the crack growth direction. Furthermore, the distance between these lines represents the increment of crack growth during a particular load excursion and hence can be compared with the macroscopic crack growth rate when striation formation is the sole operational fatigue mechanism. For this reason, the spacing between adjacent fatigue striations increases with increasing magnitude of the stress intensity factor range,  $\Delta K$ .

A second type of fracture line has been identified in many glassy<sup>(7)</sup> and some semi-crystalline polymeric<sup>(10,11)</sup> laboratory samples. Here, too, the fracture bands lie perpendicular to the direction of crack extension and increase in width with  $\Delta K$  but, unlike fatigue striations, these bands form discontinuously. It has been shown that a craze at the crack tip advances in a continuous manner over many hundreds to thousands of loading cycles before the crack suddenly strikes through the craze. Numerous studies have shown that the size of these discontinuous growth bands (DGB) corresponds to the length of the plastic zone directly ahead of the crack tip.<sup>(7,9)</sup> The latter follows from a comparison of fracture band widths at different stress intensity levels with computed values of the crack tip plastic zone dimension computed using the Dugdale formulation<sup>(12)</sup>

$$\text{Band width} \approx \text{Plastic zone width} \approx \frac{\pi}{8} \frac{K_{\max}^2}{\sigma_{ys}^2} \quad (3)$$

where  $K_{\max}$  = maximum stress intensity factor

$\sigma_{ys}$  = yield strength

From Equation 3, the computed value of  $\sigma_{ys}$  should (and does)<sup>(7)</sup> correspond to the stress for crazing.

Thus, there is at present a solid foundation of knowledge with regard to FCP response and the associated fatigue fracture micro-mechanisms of amorphous and semi-crystalline polymers. It is now appropriate to build upon this foundation by examining more clearly the response of a single polymer system to cyclic loading. In this regard, studies have been undertaken to explore the effect of material variables such as molecular weight,<sup>(13-15)</sup> molecular weight distribution,<sup>(16)</sup> external<sup>(13)</sup> and internal plasticization<sup>(15)</sup> and processing history<sup>(17)</sup> on FCP in both amorphous and semi-crystalline homopolymers and impact toughened copolymers; test variables such as cyclic frequency<sup>(18-20)</sup> and temperature<sup>(21-23)</sup> are also under consideration.

Since evidence to date shows that DGB formation as a fracture mechanism is unique to polymers, there is special interest in examining this fracture process as a function of material variables. It is known that DG bands are formed in PMMA only at low molecular weight (M) values<sup>(15)</sup> whereas DGB generation in PVC<sup>(13)</sup> occurs only above some minimum M level. Molecular weight distribution effects on DGB formation in PMMA have also been investigated.<sup>(24)</sup>

The primary objective of this thesis is to provide a further clarification of the effect of material variables on discontinuous crack growth. PVC was chosen as the polymer system for study since

clear-cut DG bands develop readily under cyclic loading and considerable FCP data have been generated for comparison. Specific objectives of this thesis include:

- 1) A completion of earlier research on the effect of molecular weight on FCP response in PVC; an examination of the effect of residual orientation on FCP response in PVC.
- 2) A determination of the effect of molecular weight, plasticizer additions and residual orientation on the discontinuous growth band fracture mechanism in PVC.
  - a) A macroscopic examination of DG bands to determine the effect of the above variables on band width, and hence the inferred  $\sigma_{ys}$ .
  - b) A microscopic examination of DG bands to observe the effect of the above variables on band morphology.

## Experimental Procedure

### Materials

The PVC specimens used in this study were obtained from two sources. Cadillac Plastics supplied extruded PVC of unspecified composition, which was found to possess an  $M_w$  of 108,000. Two series of milled and compression-molded PVC specimens were supplied by the B. F. Goodrich Co.; series 1 and 2 samples together encompassed a weight-average molecular weight from  $0.61 \times 10^5$  to  $2.25 \times 10^5$ . Samples of series 1 were prepared with varying amounts of the plasticizing agent dioctyl phthalate (DOP), while series 2 samples were studied in the unmodified state alone. The specific designation, molecular weight, plasticizer content and plaque thickness for these specimens are given in Table I.

### Characterization

Weight-average molecular weight values for series 1 and 2 were determined by B. F. Goodrich and Co. using gel permeation chromatography (GPC).  $\bar{M}_w$  determination of the extruded PVC supplied by Cadillac Plastics was also found via GPC, but by an independent source. Differential scanning calorimetry (DSC) was used to establish the glass transition temperatures of the unmodified specimens and was conducted on a Perkin Elmer instrument, Model DSC-1B, at a scan rate of  $10^\circ\text{C}/\text{min}$ . Specimen densities were measured using a density gradient column, following accepted procedures. Both the  $T_g$  and density for the unmodified specimens may be found in Table I.

TABLE I - Materials

| Series (source)   | Sample Designation | Plaque Thickness (mm) | $M_w \times 10^{-5}$ | $T_g$ ( $^{\circ}\text{C}$ ) | Density (g/cc) |
|-------------------|--------------------|-----------------------|----------------------|------------------------------|----------------|
| 1(BFG)            | A                  | 6.3                   | .605                 | 68                           | 1.411          |
|                   | A(13)*             | 6.3                   | .605                 |                              |                |
|                   | B                  | 6.3                   | .965                 | 69                           | 1.401          |
|                   | B(13)              | 6.3                   | .965                 |                              |                |
|                   | C                  | 6.3                   | 1.41                 | 71                           | 1.404          |
|                   | C(6)               | 6.3                   | 1.41                 |                              |                |
|                   | D                  | 6.3                   | 2.25                 | 72                           | 1.405          |
|                   | D(6)               | 6.3                   | 2.25                 |                              |                |
|                   | D(13)              | 6.3                   | 2.25                 |                              |                |
| 2(BFG)            | 131-1              | 6.3                   | .67                  | 67                           | 1.388          |
|                   | 132-1              | 6.3                   | .95                  | 69                           | 1.388          |
|                   | 133-1              | 6.3                   | 1.06                 | 71                           | 1.384          |
|                   | 134-1              | 6.3                   | 1.69                 | 72                           | 1.388          |
|                   | 135-1              | 6.3                   | 2.08                 | 73                           | 1.388          |
| Cadillac Plastics | CP                 | 3.2                   | 1.08                 | 53                           | 1.377          |

\* Numbers in parentheses represent the DOP content in parts per hundred of resin.

### Sample Preparation

All fatigue samples were cut in the form of compact tension coupons, with  $H/w = 0.6$  (Figure 2.) The dimensions of the Cadillac Plastics (CP) samples were 7.6 cm x 7.6 cm x 3.2 mm while series 1 and 2 samples were 7.3 cm x 7.3 cm x 6.4 mm. CP PVC samples were cut such that the loading axis was oriented at  $90^\circ$ ,  $0^\circ$ ,  $\pm 45^\circ$ , respectively, relative to the extrusion direction. Series 1 and 2 samples were cut with the load axis either  $90^\circ$  or  $0^\circ$  to the milling direction. Edge notches were machined to a depth of about 2.5 cm and then sharpened with a razor blade.

### Fatigue Testing

Fatigue tests were performed on an electro-hydraulic closed loop testing machine using sinusoidal loading and a frequency of 10 Hz. Specimen pre-cracking was conducted at 100 Hz, with the load range initially 10% higher than the eventual test range, in order to minimize total test time. After the precrack had initiated, the load range was reduced to the test range and the crack was then grown out of the chevron region a distance at least one-half the specimen thickness.<sup>(25)</sup> The R ratio ( $\frac{\text{minimum stress}}{\text{maximum stress}}$ ) was 0.1 for the majority of tests, with a limited number of tests run at  $R = 0.5$ .  $\Delta K$  was determined using equation (1). For the compact tension geometry,  $Y = 29.6 - 185.5(\frac{a}{w}) + 655.7(\frac{a}{w})^2 - 1017(\frac{a}{w})^3 + 638.9(\frac{a}{w})^4$ . Crack growth was followed with the aid of a travelling microscope and the crack length determined at roughly 0.25 mm intervals as a function of the number of load cycles  $\Delta N$ . The fatigue crack growth rate for

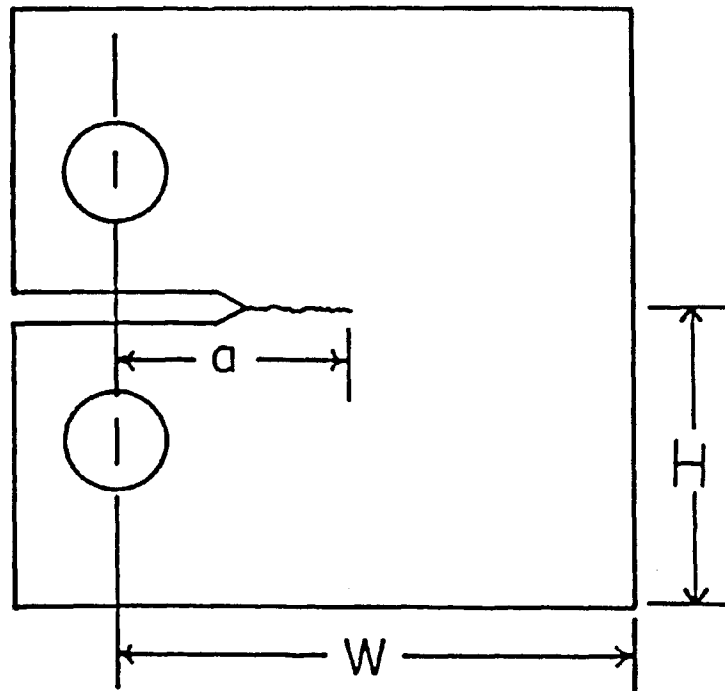


Figure 2. Compact tension specimen for generation of fatigue crack propagation data.



a crack length  $\underline{a}$  was subsequently calculated using a secant method  $\left( \frac{a_{i+1} - a_{i-1}}{N_{i+1} - N_{i-1}} \right)$  and plotted as a function of  $\Delta K$ . All tests were

performed at room temperature and in laboratory air.

#### Fractographic Examination

Fracture surface examinations were conducted on a Bausch and Lomb metallograph and an ETEC scanning electron microscope (SEM). The fracture surfaces studied in the SEM were prepared by coating with carbon and then with gold, or by coating with a gold-palladium alloy alone. It was found that an accelerating voltage of 20 kV could be employed in the SEM with little damage to the samples.

## Experimental Results and Discussion

### Fatigue Crack Propagation in PVC

#### Molecular Weight Effect

The fatigue crack growth rates in PVC as a function of  $\Delta K$  for a weight-average molecular weight ( $\bar{M}_w$ ) range of  $0.61 \times 10^5$  to  $2.25 \times 10^5$  are shown in Figure 3. This plot displays test results from three sets of PVC samples; series 1 and 2 in the unmodified state and CP PVC. All data presented in this plot were generated for samples in the  $90^\circ$  orientation and represent one sample only for each molecular weight. Overall, there is a shift to increasing growth rates with decreasing  $M$ . In addition, the slopes of each plot are all in the vicinity of  $m = 3.5 - 5$  except for sample CP ( $m = 2.4$ ).

When the growth rate is evaluated as a function of molecular weight at an arbitrary  $\Delta K$  level ( $0.7 \text{ MPa}\sqrt{\text{m}}$ ), the results from series 2 and the CP PVC are found to be in good agreement with the curve originally determined from series 1 data alone (Figure 4). These results reinforce the previously proposed relationship that describes the fatigue crack growth rate  $da/dN$  as varying directly with  $\exp(1/M)$  (Figure 5).<sup>(13)</sup> The data clearly reveal the dependence of the fatigue crack growth rate on  $\exp(1/M)$ . Note that this relationship also describes the effect of  $M$  on  $da/dN$  in PMMA as well.<sup>(15)</sup>

From Figure 4, it is seen that the dependence of FCP

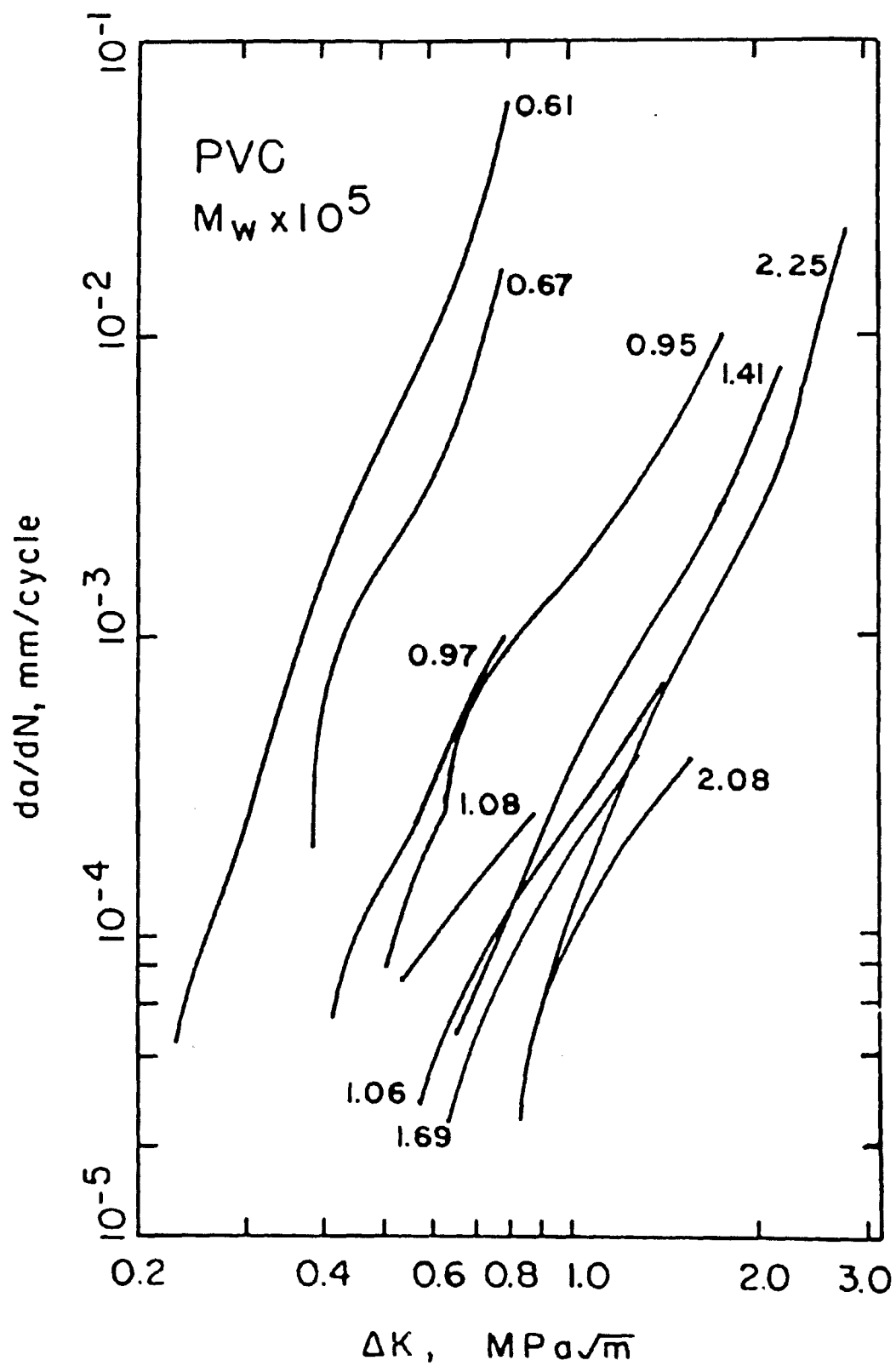


Figure 3. Effect of molecular weight on fatigue crack propagation of PVC;  $R = 0.1$ , 10 Hz ( $CPM_w = 1.08 \times 10^5$ ).

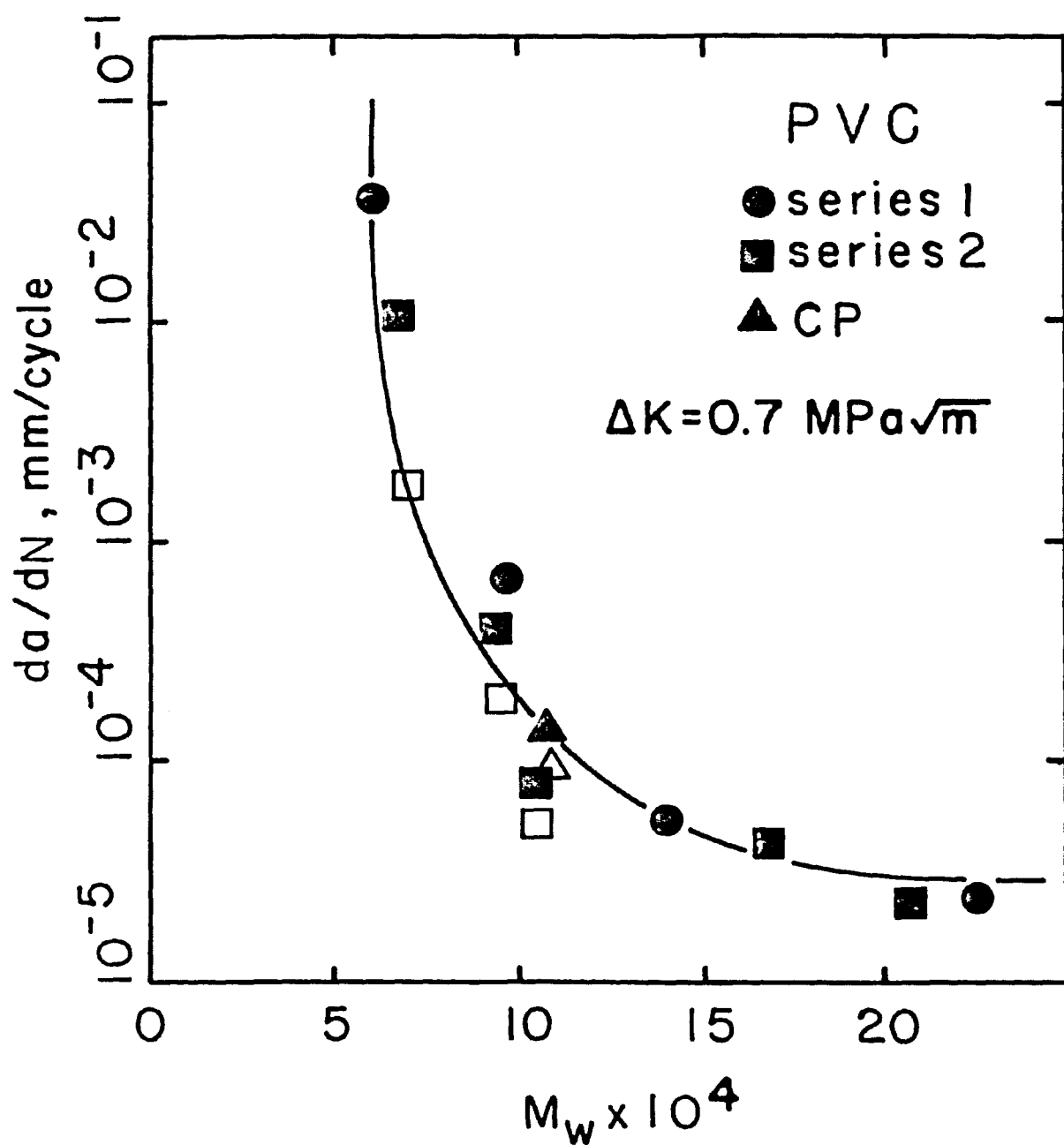


Figure 4. Effect of molecular weight and orientation on the fatigue crack growth rate of PVC. (● ■ ▲) = 90°, (○ □ △) = 0° test orientation.

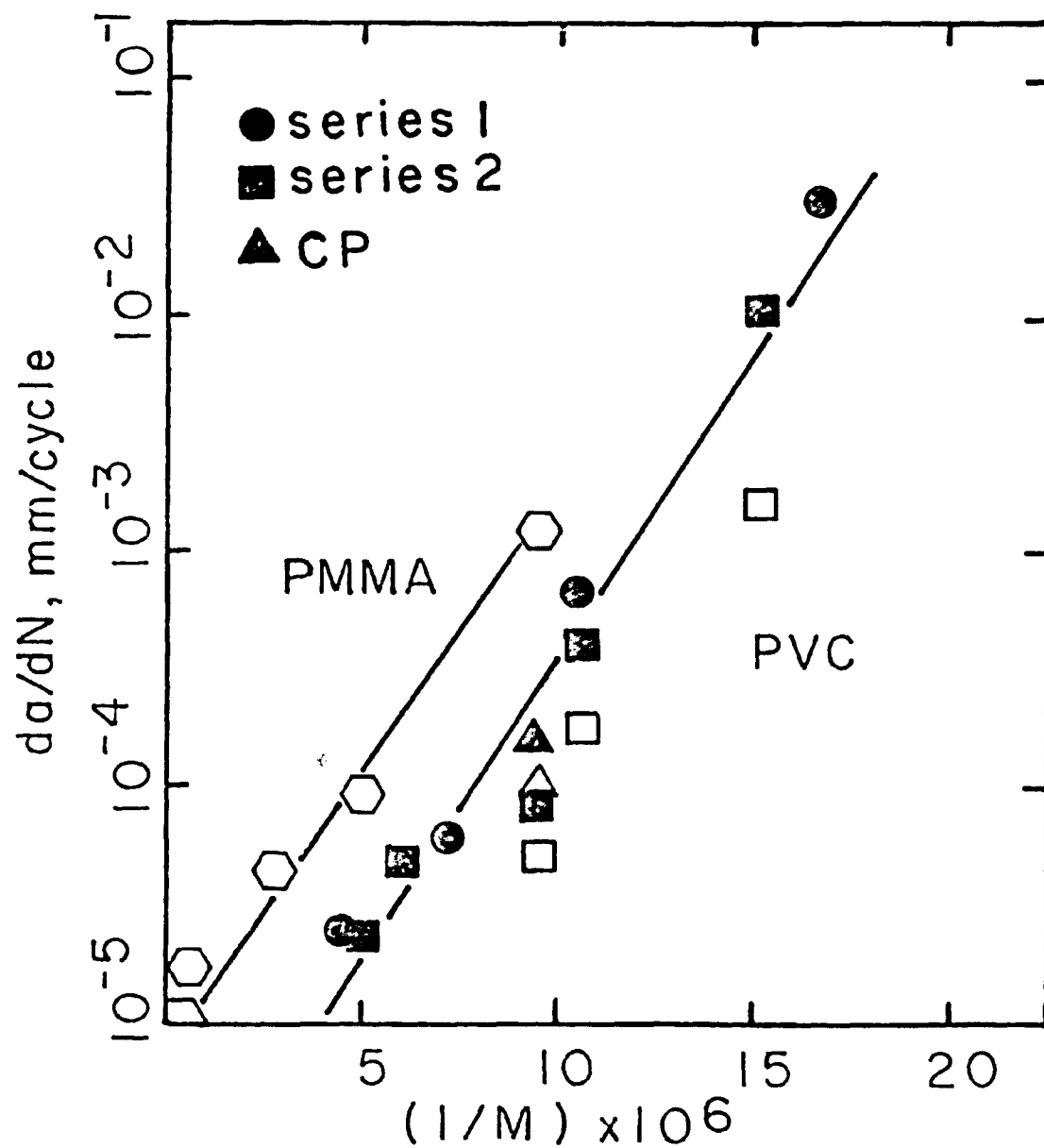


Figure 5. Relationship between FCP rate and  $1/M$  for PVC ( $\Delta K = 0.7 \text{ MPa}\sqrt{\text{m}}$ ) and PMMA ( $\Delta K = 0.6 \text{ MPa}\sqrt{\text{m}}$ ).  
 (● ■ ▲) =  $90^\circ$ , (○ □ Δ) =  $0^\circ$  test orientation.

resistance on molecular weight varies with molecular weight itself. In all cases, higher M leads to a lowering of fatigue crack growth rates at a given  $\Delta K$  level; the strength of this dependence, however, diminishes with increasing M. For example, a doubling of M from  $0.6 \times 10^5$  to  $1.2 \times 10^5$  results in an approximately 200 to 300-fold decrease in FCP rates, whereas doubling M again reduces crack growth rates by only three to four times. It would appear then that any further increase in M of these PVC samples would have little influence on the material's fatigue response and that the lowest obtainable FCP rate in PVC could be represented by an asymptotically limiting value as a function of molecular weight.

The observation that FCP resistance increases up to some limiting value is not surprising in light of the fact that static properties of polymers (modulus,  $T_g$ , tensile and yield strength) are a function of M and also reach a limiting value at some molecular weight. However, the M at which the plateau for static properties is attained is generally lower than that for FCP resistance. Therefore, even though maximum static properties may be achieved at a relatively low M, there still remains room for improvement in the fatigue resistance of PVC with further increase in molecular weight. The reason for the higher M required for fatigue property saturation is believed to be related to the different deformation response of polymeric materials to cyclic vs static loading. For example, repeated loadings will induce chain disentanglement and bring about more overall weakening of the polymer than would a

single load application of the same magnitude. Consequently, a higher M (and associated greater degree of chain entanglement) is needed under cyclic loading conditions to maintain equivalent polymer resistance to stress induced damage.

#### Residual Orientation Effect

Anisotropic fatigue and fracture behavior has been noted in many wrought metal alloys. It is appropriate, therefore, to investigate the effect of residual orientation due to processing on the fatigue behavior of polymers. In fact, it was recently reported that the fracture toughness of injection-molded polypropylene varied by nearly a factor of two with change in specimen orientation.<sup>(26)</sup>

The effect of residual orientation in compression-molded PVC was studied using series 2 plaques tested with the load axis both  $0^\circ$  and  $90^\circ$  to the original milling direction. Returning to Figure 4, it is seen that at this stress intensity level the growth rates at each molecular weight for the  $0^\circ$  (longitudinal) samples are either equal to or lower than those recorded for the  $90^\circ$  (transverse) specimens.

Samples 134-1 and 135-1 show identical growth rates in the two orientations. However with decreasing M, one finds a factor of two difference in FCP rates in samples 132-1 and 133-1 and a factor of three difference in growth rates between the  $0^\circ$  and  $90^\circ$  orientations for sample 131-1.

It is possible that these results may simply reflect normal test scatter since a factor of two difference in crack growth rate

can be attributed to experimental error in reading the length of the advancing crack tip.<sup>(27)</sup> Therefore, the two to three fold difference in FCP rates as a function of orientation in compression molded PVC merely borders on being a significant observation. However, since there is a consistently increasing difference in growth rates between  $90^{\circ}$  and  $0^{\circ}$  samples with decreasing M, the effect of orientation on  $da/dN$  is considered to be real, albeit slight.

At each molecular weight one may expect some residual chain alignment and more effective chain entanglements in the  $0^{\circ}$  (or milling direction) sample orientation. Superimposed on this directionality is the overall number of chain entanglements which increases with increasing M. Hence, at low M, where the total chain entanglement density is not great, residual anisotropy in entanglements can produce a slight difference in FCP behavior in the two orientations. Conversely, the much higher density of chain entanglements at high M is thought to be sufficiently great so as to render insignificant any second order chain entanglement directionality. Note that this hypothesis is consistent with the overall trend of FCP dependence on molecular weight: a small difference in M at low M values would be expected to have a measurable influence on fatigue behavior while the same would not be true at high molecular weights.

Attention was next given to an analysis of fatigue response in the CP plaques to determine whether more pronounced directionality might be present in this extruded material supply as compared to the milled and compression-molded specimens. Recall that CP



plaques were cut with the load axis  $90^{\circ}$ ,  $0^{\circ}$  and  $\pm 45^{\circ}$  to the extrusion direction. Plots of  $da/dN$  vs  $\Delta K$  for the four orientations and at R ratios of 0.1 and 0.5 are shown in Figures 6a and b, respectively. Crack growth rate differences of about a factor of two are noted which could be attributed to experimental error. But, as was observed with the compression-molded PVC, those samples loaded  $90^{\circ}$  to the direction of residual orientation again exhibited the lowest FCP resistance (and, in this case, the lowest maximum recorded  $\Delta K$  value).

It is not surprising that the  $90^{\circ}$  orientation samples have the highest growth rates and lowest toughness since the crack plane is oriented parallel to the extrusion direction. Some chain alignment is expected in this direction, which would result in less stable craze development ahead of the crack tip. The growth rates for the remaining three test orientations are similar. However, the  $-45^{\circ}$  samples do exhibit slightly better fatigue resistance than the  $0^{\circ}$  and  $45^{\circ}$  orientation specimens at both mean stress levels, especially at high  $\Delta K$  values. In conclusion, a slight, but consistent effect of residual orientation on FCP resistance appears to exist for both extruded and compression-molded PVC. In both materials, fatigue tests conducted with the load axis transverse to any residual molecular orientation yields the least resistance to cyclic crack growth.

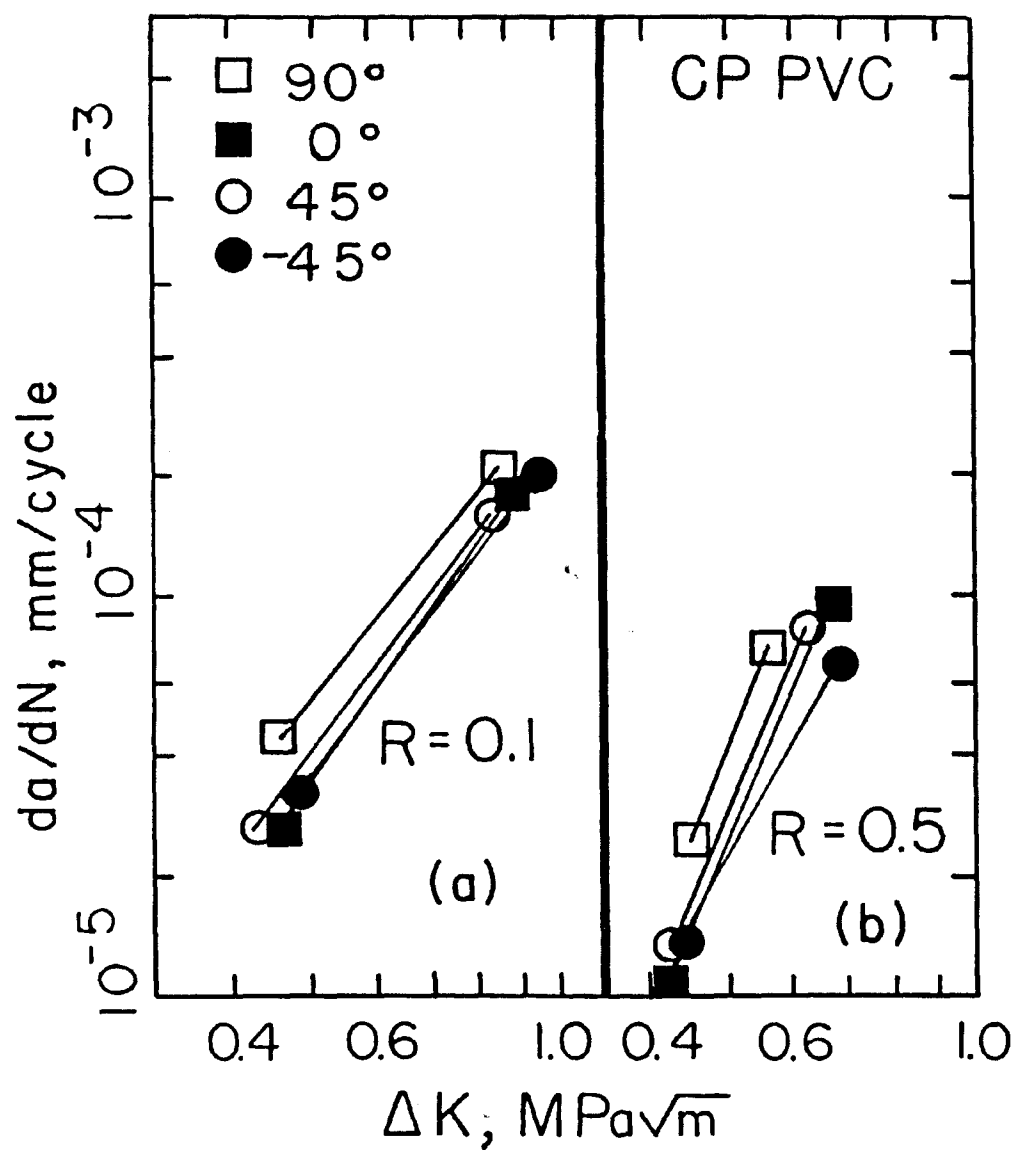


Figure 6. Effect of orientation and mean stress on FCP behavior in CP PVC ( $M_w = 1.08 \times 10^5$ ).

## Fractographic Analysis of PVC

### Macromorphology

Unmodified samples from the series 1 and 2 material supply were used to study the effect of molecular weight on the fatigue fracture morphology. All samples having molecular weights in the range between  $M_w = 0.95 \times 10^5$  and  $M_w = 2.25 \times 10^5$  failed by discontinuous crack growth. In sharp contrast, specimens with weight-average molecular weights of  $0.61 \times 10^5$  and  $0.67 \times 10^5$  showed no evidence of DGB formation and presumably failed by some continuous cracking process. Furthermore, in all but one case, DG bands were found to extend over the entire fatigue fracture region of these samples. The exception was sample 132-1 from series 2 ( $M_w = 0.95 \times 10^5$ ), which revealed DG bands only at low values of  $\Delta K$ ; fatigue striations were observed at high  $\Delta K$  levels.

Measurements of band sizes were made from all samples and compared with corresponding  $\Delta K$  levels. The results are presented for series 1, 2 and CP PVC in Figures 7, 8 and 9, respectively. A composite of the above plots, with the data being represented by least squares fit lines, is given in Figure 10. Note that the results from samples B to D and 132-1 to 135-1 all lie within a relatively narrow scatter band, revealing no clear effect of molecular weight on DG band size. On the other hand, the band spacings associated with the CP samples were consistently larger than those found for series 1 and 2.

The logarithmic slopes of band size vs  $\Delta K$  data for these samples are similar ( $1.7 \pm 0.2$ ) and are in reasonably good agree-

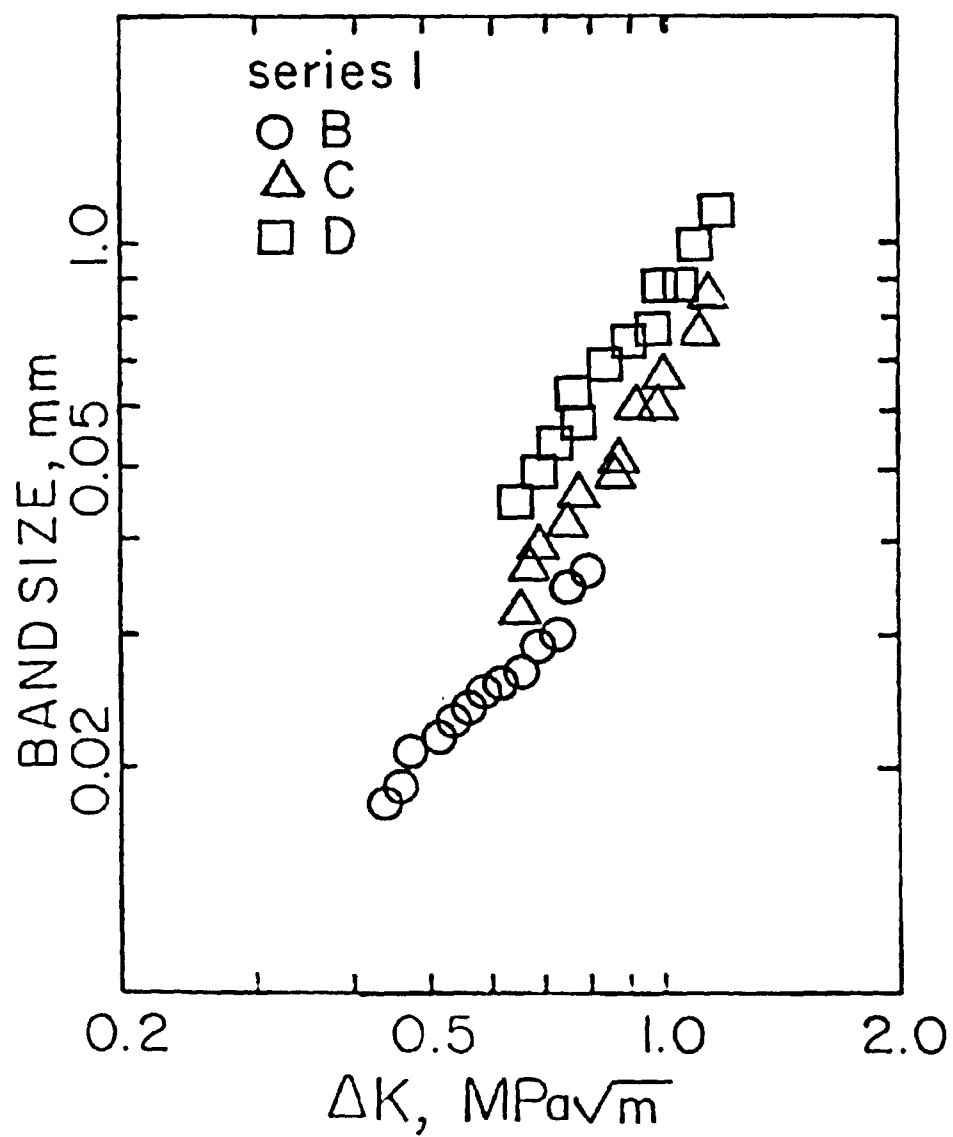


Figure 7. Discontinuous growth band size as a function of  $\Delta K$  for Series 1 PVC.

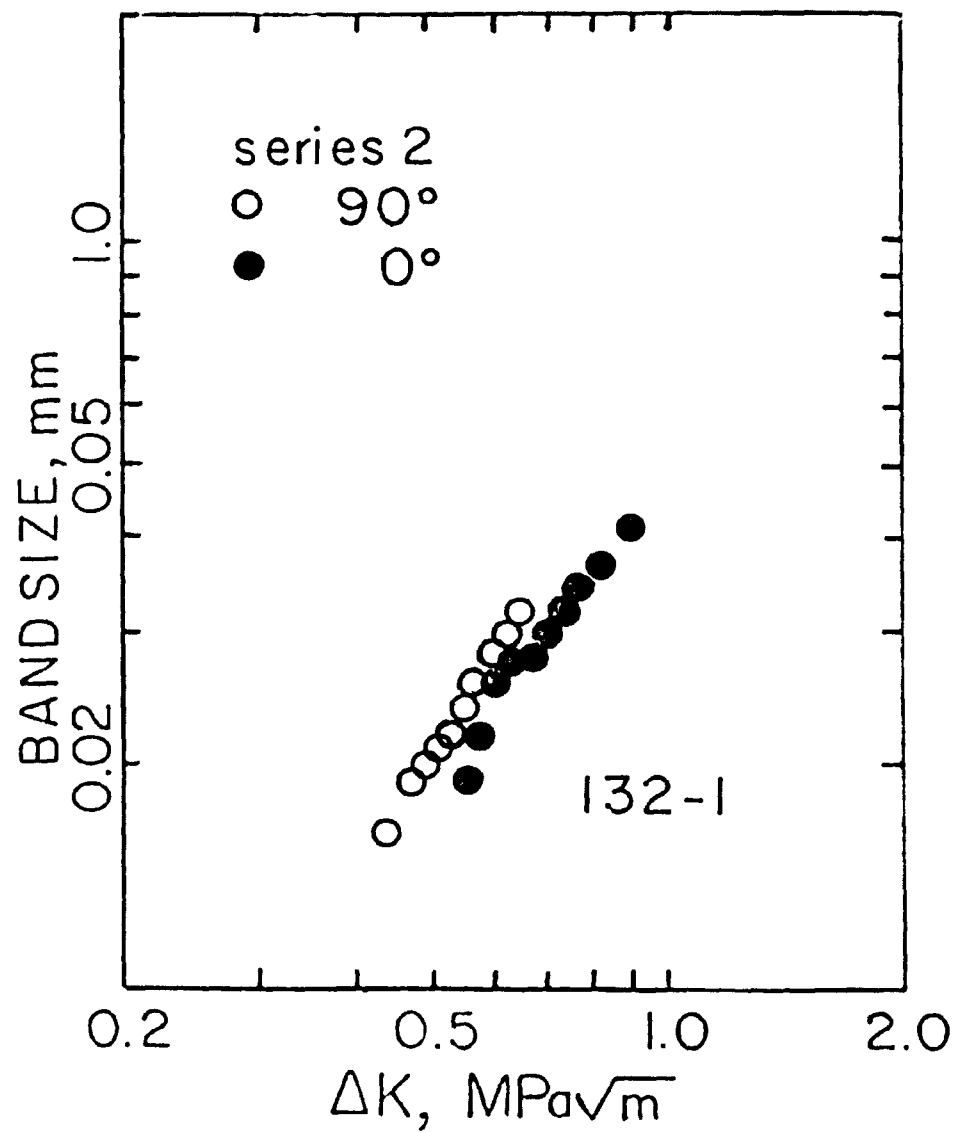


Figure 8. DG band size as a function of  $\Delta K$  and test orientation for Series 2 PVC. (a) 132-1

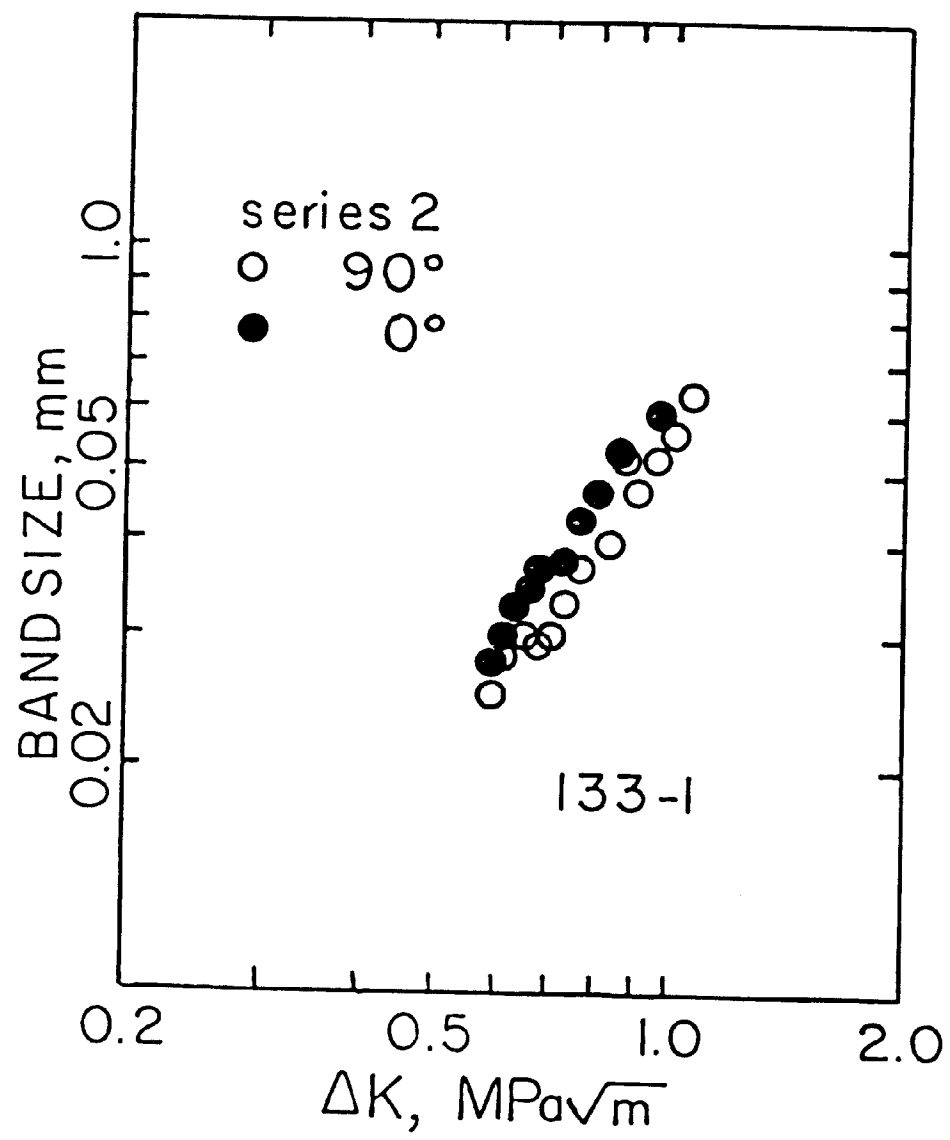


Figure 8. (b) 133-1

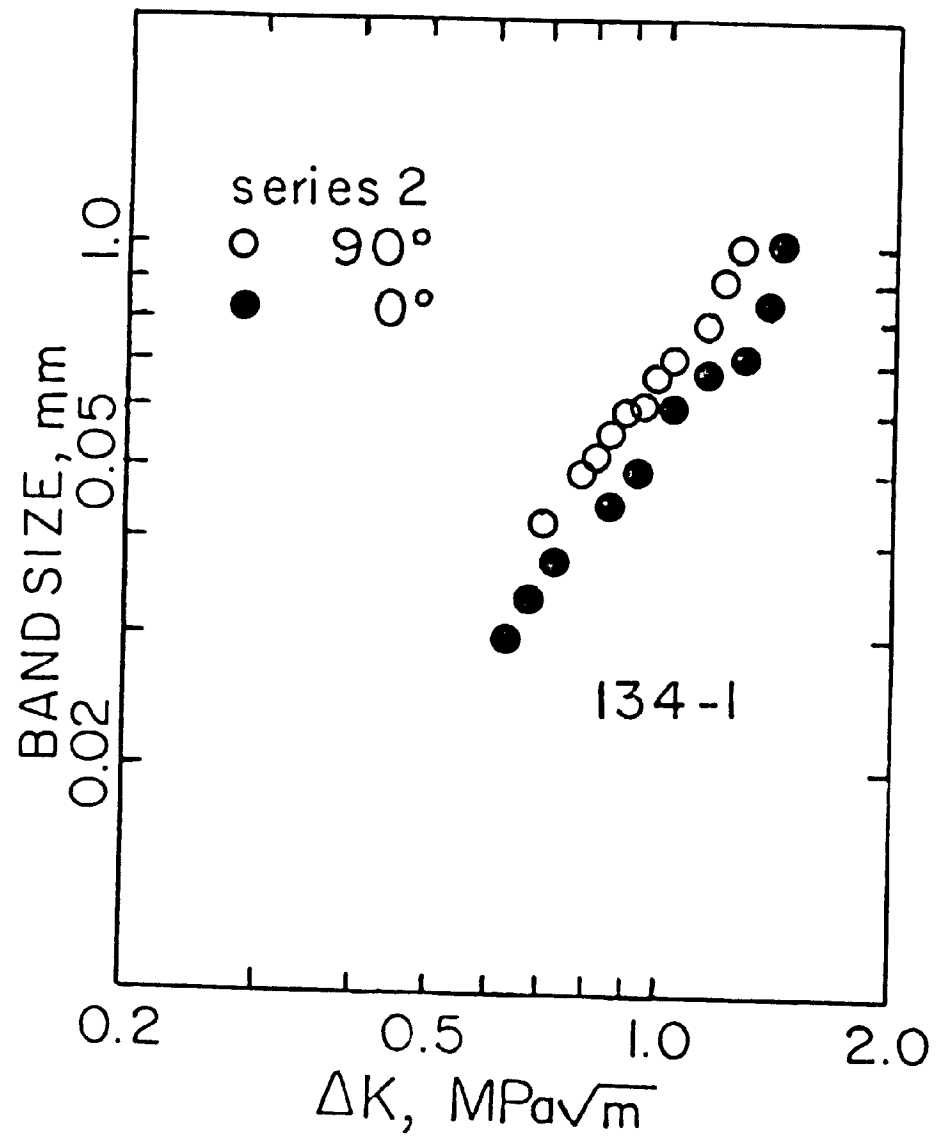


Figure 8. (c) 134-1

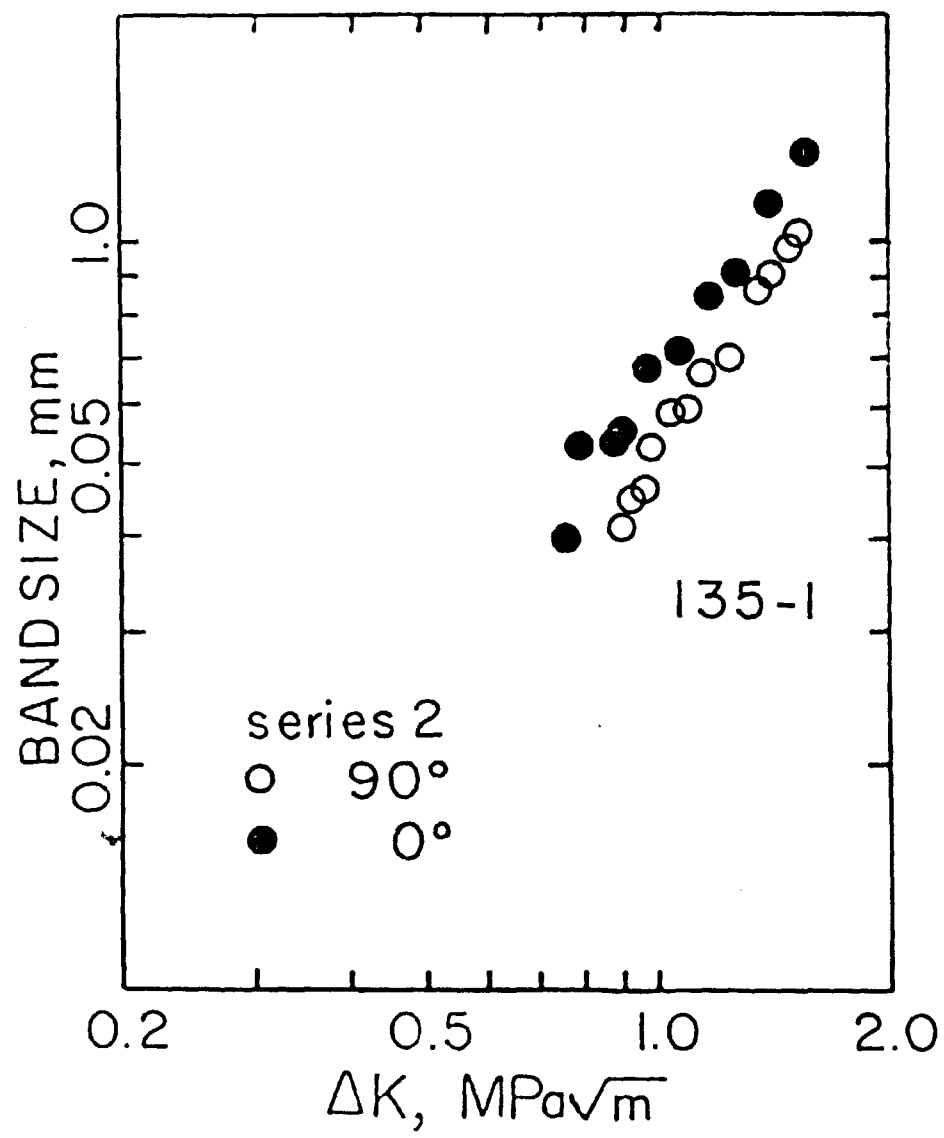


Figure 8. (d) 135-1



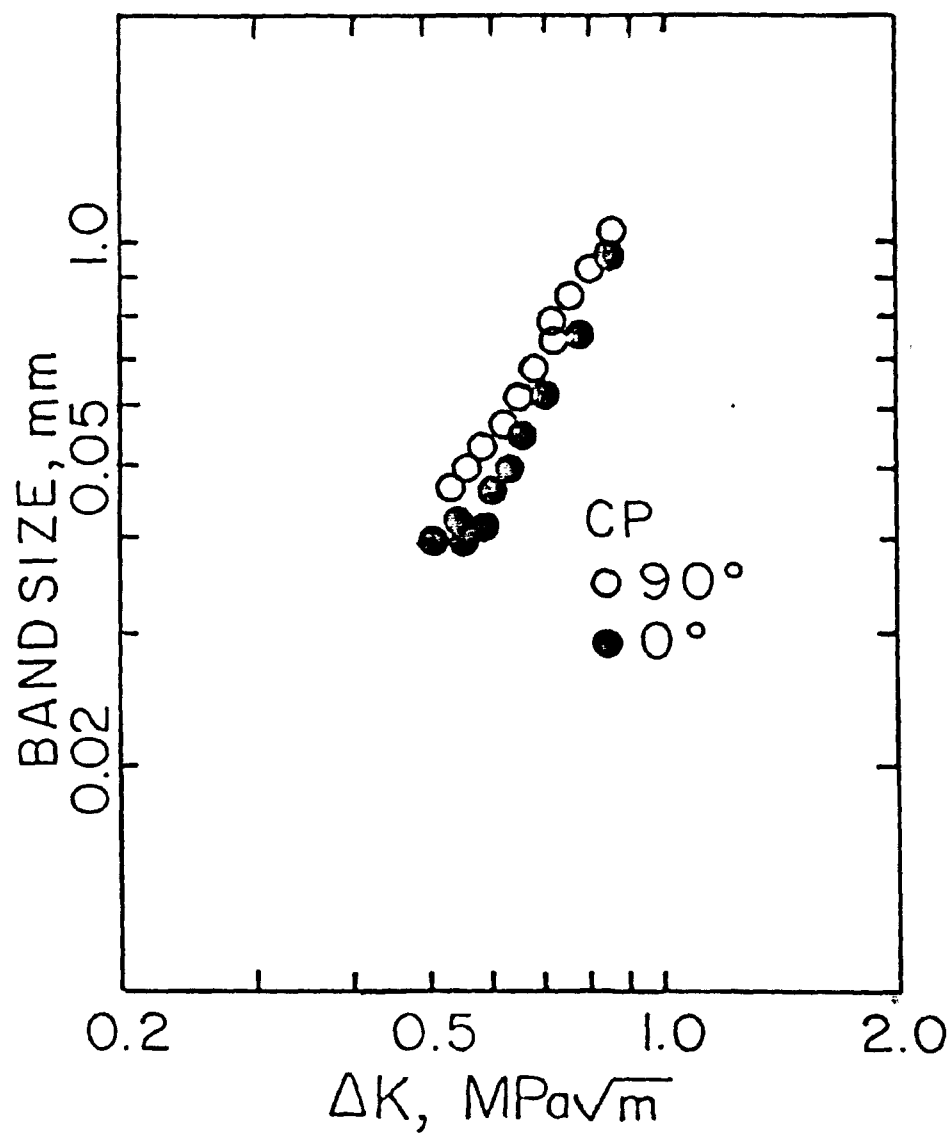


Figure 9. DC band size as a function of  $\Delta K$  and test orientation for CP PVC. (a) 90°, 0°

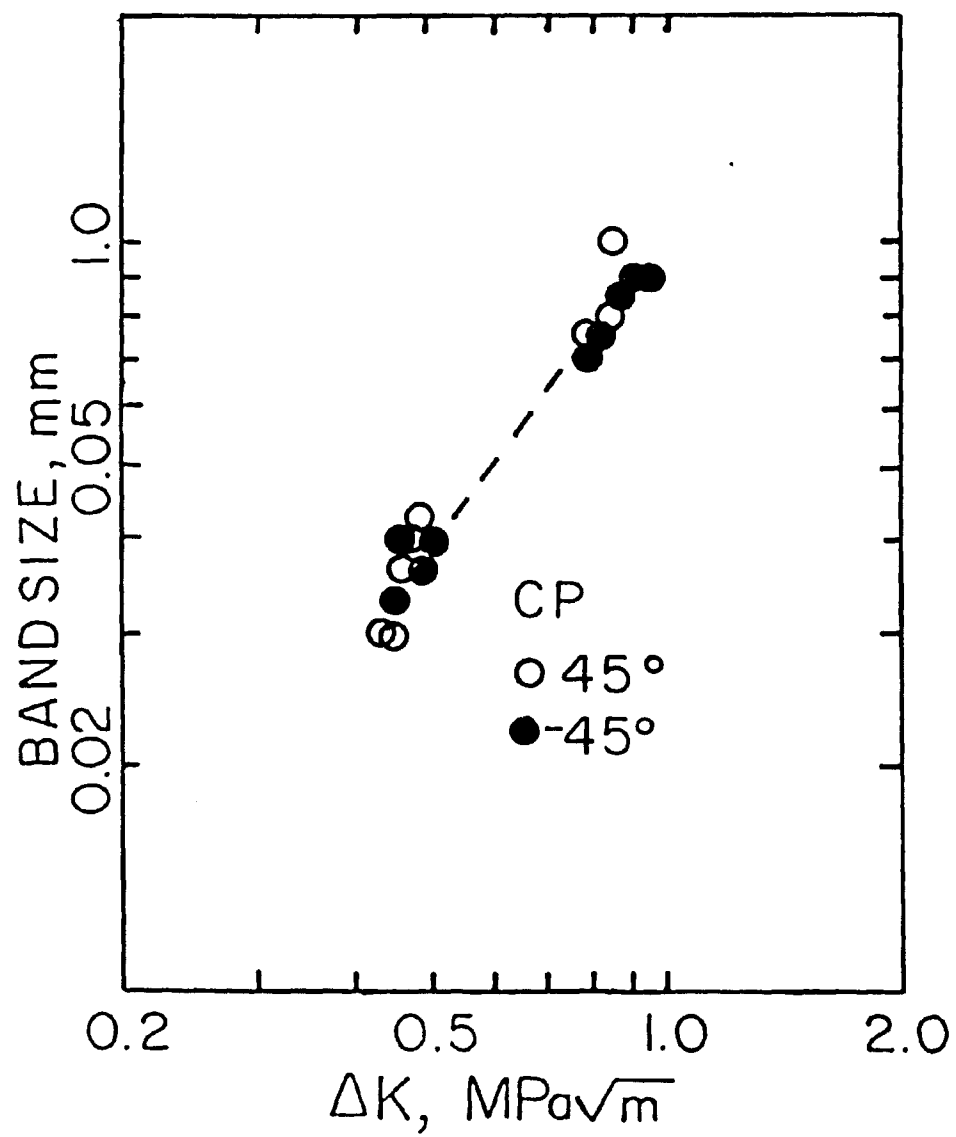


Figure 9. (b) +45°, -45°

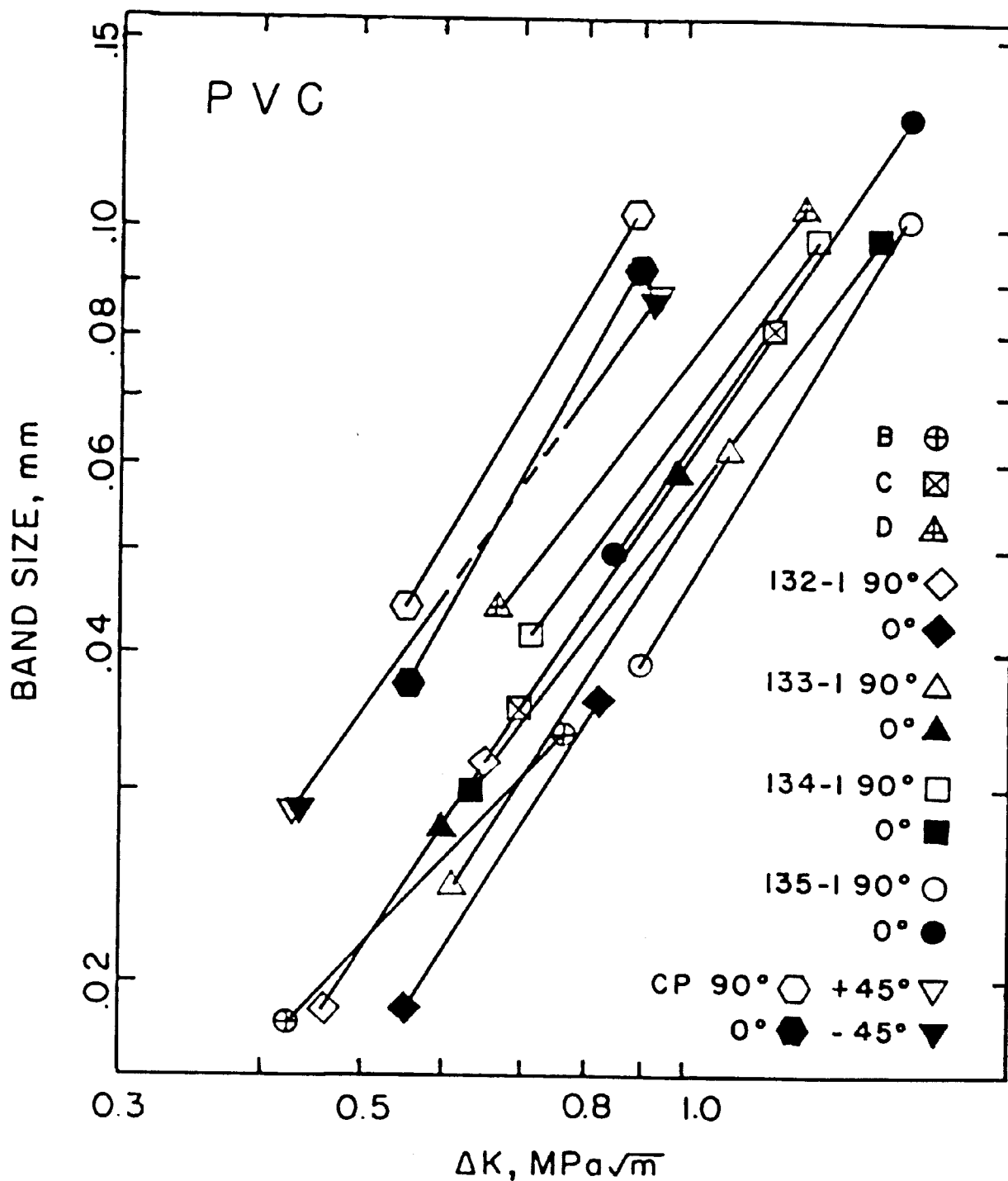


Figure 10. Discontinuous growth band size as a function of  $\Delta K$  and test orientation for PVC. No DG bands observed below  $M_w = 0.95 \times 10^5$ .

ment with the second power relationship of  $K_{\max}$  to the plastic zone size, as proposed in the Dugdale model.<sup>(12)</sup> Consequently, equation 3 was used to calculate an inferred yield strength for these materials at different  $\Delta K$  values over the test range (see Table II). The inferred yield strengths for specimens B, C and D from series 1 varied from 70 to 80 MPa while yield strength values from samples 132-1 to 135-1 from series 2 ranged from 75 to 85 MPa. These values are somewhat higher than those reported by Mills<sup>(28)</sup> who found an upper yield strength of 65 MPa in rigid PVC when tested at a strain rate of  $10^{-4} \text{ sec}^{-1}$ . Since the strain rate associated with fatigue testing at 10 Hz is surely several decades higher than that employed by Mills, one would expect the inferred yield strength, derived from these fatigue experiments, to be higher. In fact, using a yield strength-strain rate dependency in PVC of approximately 6 MPa per decade change in strain rate, as determined from results generated by several investigators,<sup>(29-32)</sup> the 10 to 15 MPa difference between yield strength values reported by Mills and inferred in this study from fractographic measurements would correspond to a two to three fold difference in strain rates used in these two studies. This difference seems reasonable based upon some preliminary computations of the strain rate at the crack tip. Overall, the inferred yield strengths for these samples varied little with molecular weight--a finding consistent with the lack of dependence of yield strength on molecular weight for this range of  $M_w$  values.<sup>(33,34)</sup>

Recall that series 2 samples were tested with the load axis both parallel ( $0^\circ$ ) and perpendicular ( $90^\circ$ ) to the milling

TABLE II - Calculated Yield Stresses for  
CP and Series 1 and 2 Using  
the Dugdale Model<sup>a</sup>

| Series | DOP, % | $\sigma_{ys}^b$ , MPa |
|--------|--------|-----------------------|
| 1      | 0      | 70-80 <sup>(13)</sup> |
| 1      | 6      | 56                    |
| 1      | 13     | 40                    |
| 2      | 0      | 75-85                 |
| CP     | ?      | 53-61 <sup>(7)</sup>  |

<sup>a</sup>In all cases  $R \left( \frac{\sigma_{min}}{\sigma_{max}} \right) = 0.1$

<sup>b</sup>An average

direction. Examination of these samples showed that the fracture mechanisms operative at each M were fundamentally the same, regardless of orientation. That is, sample 131-1 revealed no DG bands in either test orientation, while samples 132-1 to 135-1 revealed DG bands in both test orientations. Referring again to Figures 8a-d, it appears that, while there are small differences in DGB width with orientation at each molecular weight, a trend is not well-defined.

The effect of residual orientation on DGB formation in the extruded CP PVC (tested with the load axis at  $0^\circ$ ,  $90^\circ$  and  $\pm 45^\circ$  to the extrusion direction) is somewhat more complicated. The  $90^\circ$  sample shows DG bands across the entire width of the fracture surface and at all stress intensity levels up to fast fracture. The other 3 orientations have a rough, "mist" region in the interior of the fracture surface in the intermediate  $\Delta K$  range ( $\sim 0.47$  to  $0.75$  MPa $\sqrt{m}$ ). This mist region interrupts DG band formation either mildly ( $0^\circ$ ) or strongly ( $\pm 45^\circ$ ). A similar mist region has been noted on the fracture surfaces of polycarbonate and polysulfone<sup>(7)</sup> and is believed to be the result of the crack growing through multiple crazes, rather than a single craze, during fatigue crack growth. The reason for this transient behavior in some CP samples is not clear at this time. Band size measurements for these samples are shown in Figure 9a,b. [For the  $\pm 45^\circ$  samples, measurements were made only at those  $\Delta K$  values where the DG band extended across the entire fracture surface width (i.e., at low and high  $\Delta K$ ).] The results show that the  $90^\circ$  orientation sample possessed the largest band size at a given  $\Delta K$ , implying that the yield strength is lowest in

this testing direction.

When a plasticizing agent is added to PVC, the yield strength of the polymer is usually lowered. As expected, the presence of 6% and 13% DOP in series 1 samples reduced the inferred yield strength by 25% and 47%, respectively (Table II). This reduction in yield strength leads to an increase in DGB width (Figure 11). Finally, the larger DGB spacings in the CP samples (Figure 10) translate to a lower inferred yield strength--an observation suggesting a significant degree of plasticization in these specimens.

Since a DG band is developed over many loading cycles, the cyclic stability or life of each band  $N^*$  may be determined by dividing the band width by the corresponding fatigue crack growth rate so that

$$N^* = \frac{\text{Band Width}}{da/dN} \quad (4)$$

From Figure 12 it is seen that  $N^*$  depends strongly on the stress intensity factor range; in all cases, the number of loading cycles necessary to strike through the craze decreases as  $\Delta K$  increases. This is attributed to the greater amount of cyclic damage introduced within the craze zone at the higher  $\Delta K$  levels. Of particular significance, the overall craze stability is seen to improve with increasing molecular weight and is quite consistent with the markedly greater degree of fatigue crack propagation resistance observed with high M samples (Figure 3). The largest improvement in craze stability is found by increasing M in the low M regime, with craze stabil-

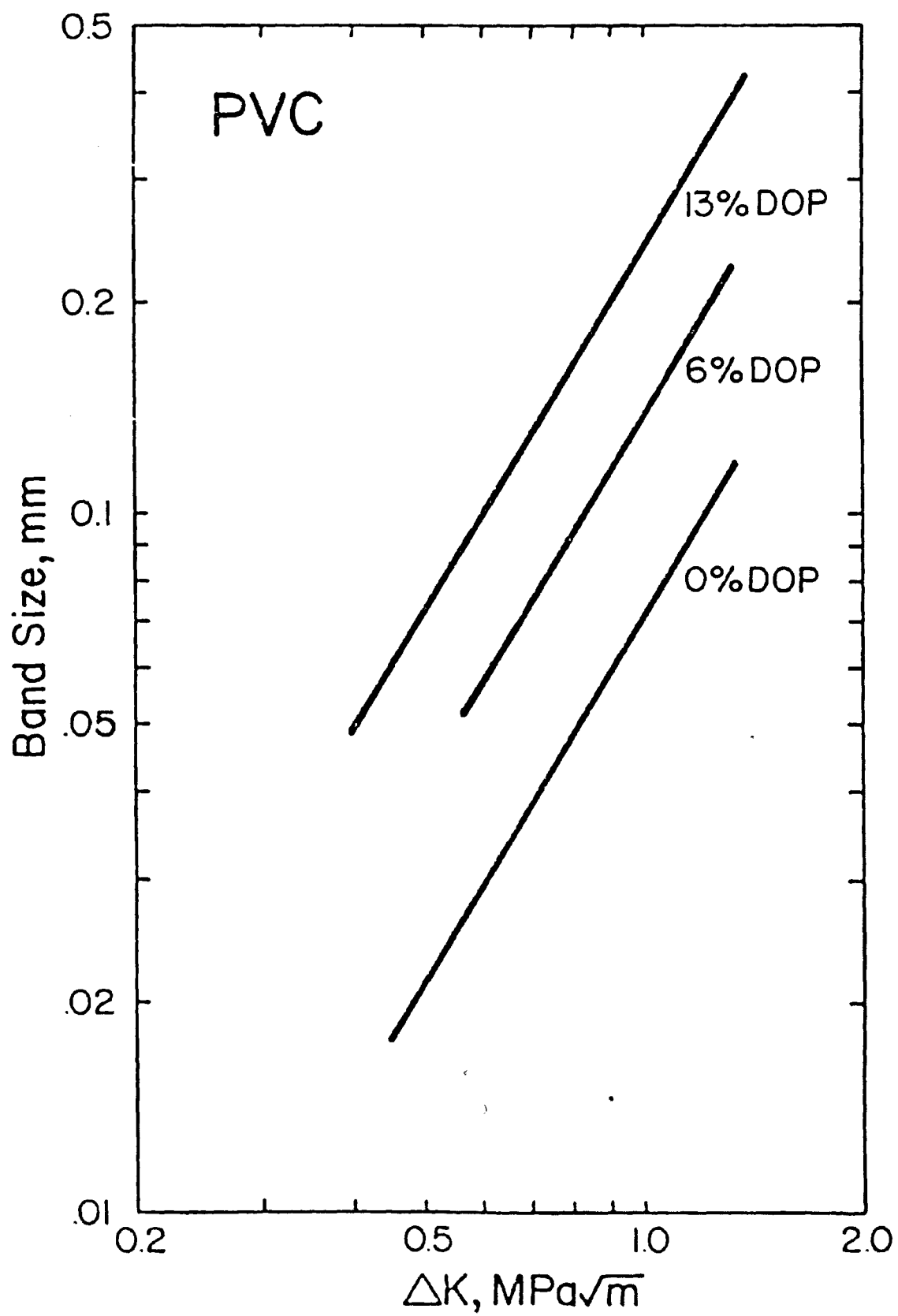


Figure 11. Effect of DOP content on DG band sizes of PVC. <sup>(13)</sup>



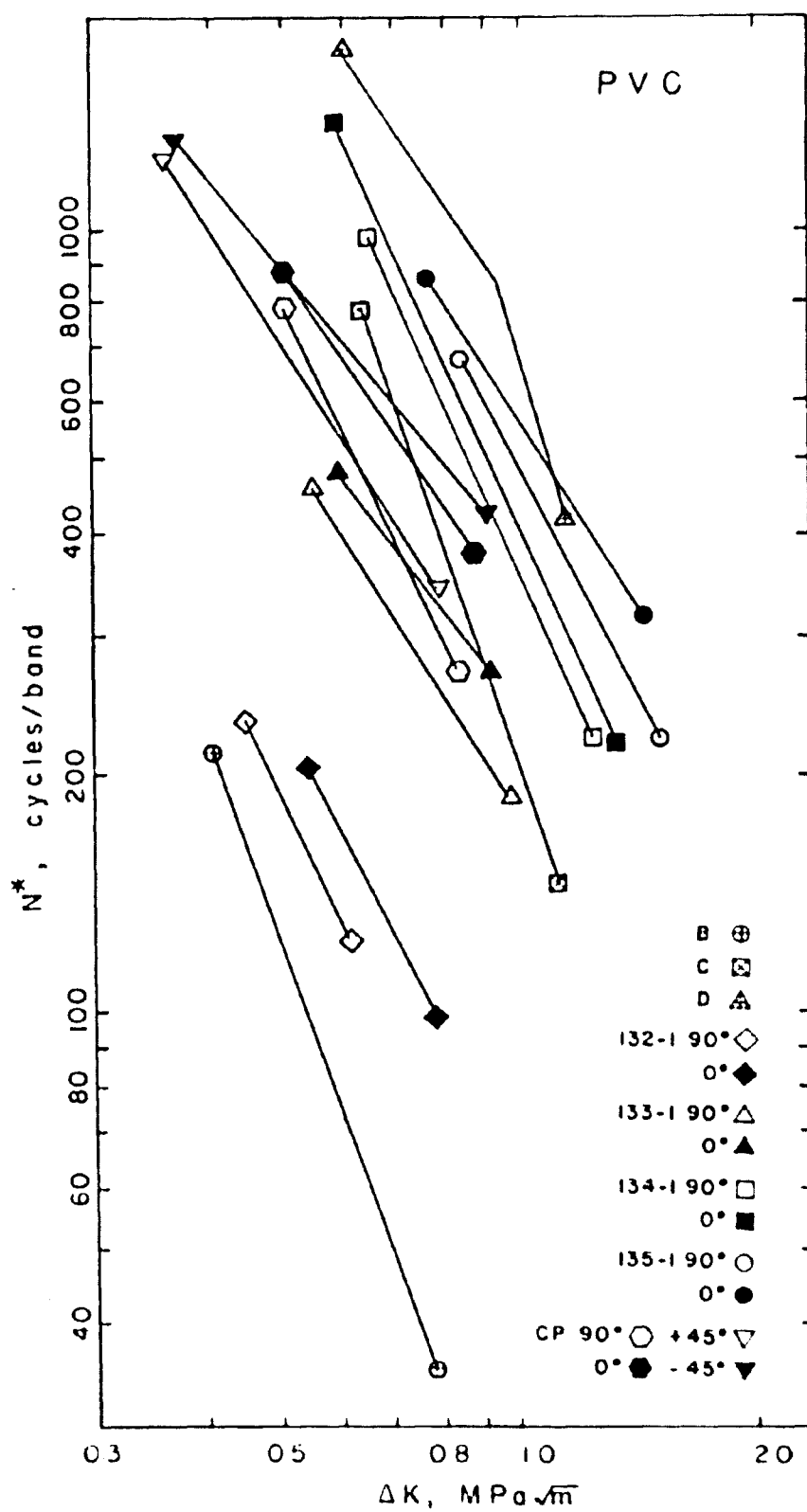


Figure 12. Effect of molecular weight on cyclic stability ( $N^*$ ) of crazes in PVC as a function of  $\Delta K$  and test orientation.

ity tending to reach some limiting value at high M levels. This saturation in craze stability at high molecular weights is to be expected because the improvement in FCP response likewise reaches a limiting growth rate plateau at high M (see Figure 4). That is, since DGB widths do not change significantly with M and the growth rate approaches an asymptotic value at high molecular weights,  $N^*$  tends toward a limiting level for a given  $\Delta K$  (see Equation 4 and Figure 13).

With regard to the effect of residual orientation on the cyclic stability of series 2 samples, a relationship is revealed between craze stability  $N^*$  and test orientation (Figure 12). DG bands produced in  $0^\circ$  samples tend to be slightly more stable than those found on the  $90^\circ$  samples. Consequently, for this series of milled and compression-molded PVC samples, test orientation does not have a pronounced effect on the inferred yield strength, but does affect craze stability. When the test is conducted such that the loading axis is parallel to the original milling direction, the crazes have a small but consistently greater stability at all molecular weights. The extruded CP material also reveals that craze stability is greater for the  $0^\circ$  orientation sample as compared with that found for the  $90^\circ$  specimen. (At this time, the difference in craze stability associated with the  $\pm 45^\circ$  samples cannot be explained). Overall, the improved craze stability in the  $0^\circ$  test orientation for both series 2 and CP samples is in agreement with the presumed existence of a mill-induced directionality with chain entanglements, as discussed earlier.

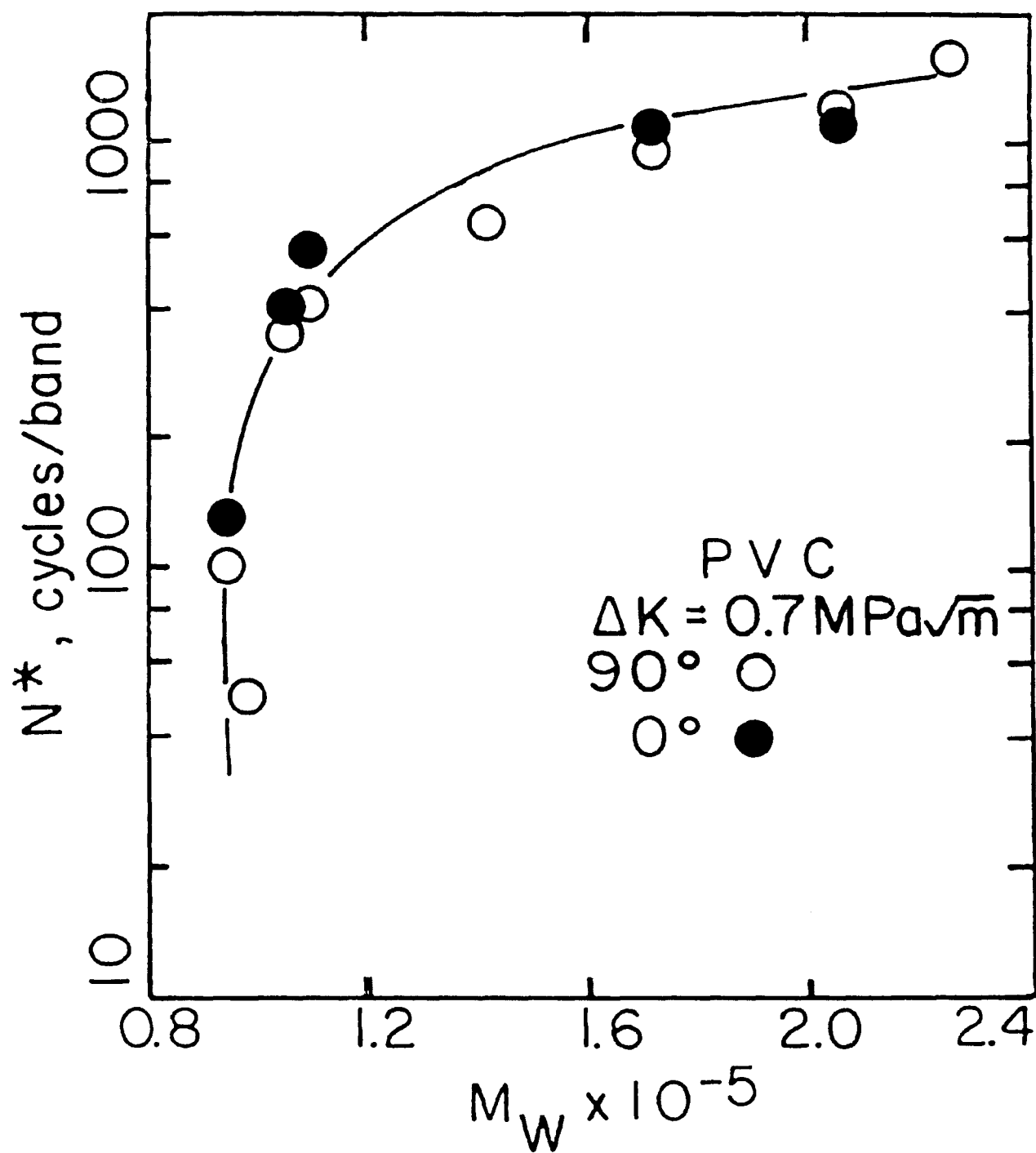


Figure 13. Cyclic stability ( $N^*$ ) as a function of molecular weight ( $M_w$ ).

Finally, the cyclic stability of DG bands in the plasticized material is greater than that of the unplasticized materials. This arises from the fact that the FCP resistance of PVC over the molecular weight range studied is little affected by plasticizer content.<sup>(13)</sup> Consequently,  $N^*$  should increase with plasticizer content since the band size increases (Figure 12) while  $da/dN$  remains essentially unchanged. For this same reason, the cyclic life of the DGB in the CP material supply is greater than DGB life in sample 133-1 even though the molecular weight is the same in these two materials. The cyclic stability of the DOP-plasticized samples follows a similar trend when compared to their unmodified counterparts (Figure 14);  $N^*$  increases with increasing DOP content for the three molecular weights studied. The change in relative ranking between samples D (6) and D (13) is attributed to the lower FCP rates exhibited by specimen D (6) (recall Equation 3).

#### Micromorphology

When DG bands are examined in the SEM at increased magnification, some general trends in micromorphology become apparent as a function of  $\Delta K$ , molecular weight and plasticizer content. Each discontinuous growth band reveals an array of microvoids which decrease in size in the direction of crack growth. These microvoids reflect the passage of the fatigue crack through the mid-region of the porous craze zone. As discussed earlier, a DG band is formed over many loading cycles so that the craze accumulates an additional increment of damage with each loading cycle. A gradual breakdown of molecular entanglements results, along with the nucleation and growth

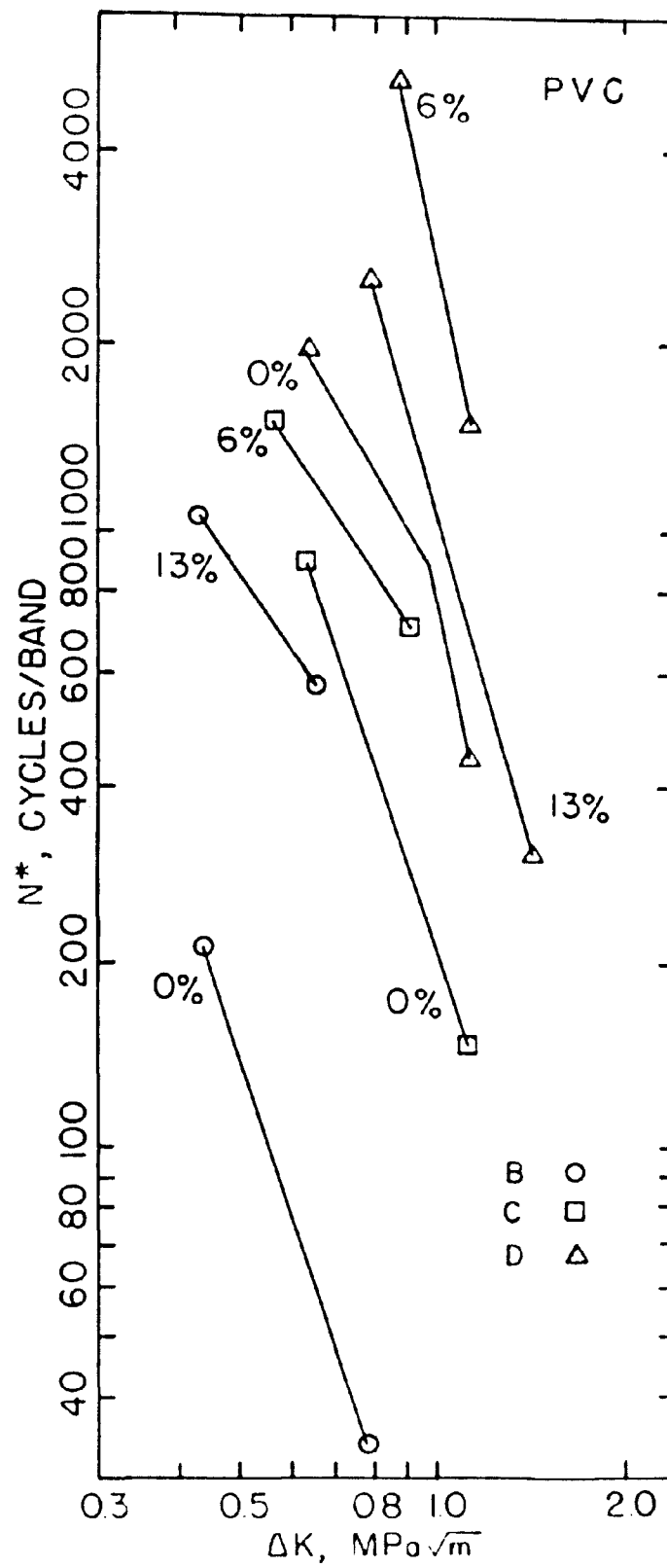


Figure 14. Effect of DOP content on cyclic stability ( $N^*$ ) of crazes in PVC as a function of  $\Delta K$ .

of microvoids. It is believed that the size of the voids depends on the magnitude of the crack tip opening. Since this displacement decreases with increasing distance from the crack tip, the resulting voids should vary in size in similar fashion. Figure 15 illustrates this by showing the last half of one DG band (small voids) and the beginning of the next DG band (large voids). The darker band which separates these two contiguous bands is referred to as the stretch zone and represents the region of crack blunting associated with crack arrest as the crack suddenly encounters initially uncrazed polymer material.

At lower molecular weights ( $M_w = \sim 0.95 - 1.10 \times 10^5$ ), as  $\Delta K$  increases the stretch zone width increases relative to the overall band size (Figure 16a,b). Since the crack opening displacement is directly related to  $K_{max}^2$  ( $COD = K_{max}^2 / E \sigma_{ys}$ ), one would expect crack tip blunting to be greater at higher stress intensity levels.

At higher molecular weights ( $M_w = \sim 1.4 - 2.25 \times 10^5$ ) the DG bands become less well-defined. As is seen in Figure 17 for sample 134-1 ( $M_w = 1.69 \times 10^5$ ), the void gradient no longer reveals a smooth transition from large to small voids. Also, while the stretch zone is still apparent at high  $\Delta K$  for this molecular weight, it is not a distinct feature of the band. That is, the large voids seem to be "overlapping" into the stretch zone. Finally, an examination of the highest M sample of series 2 ( $M_w = 2.08 \times 10^5$ ) reveals that the stretch zone is completely obscured by large voids and that no clear void gradient can be distinguished (Figure 18a).



Figure 15. SEM fractograph showing void gradient and stretch zone associated with adjacent DG bands. Arrow indicates direction of crack growth,  $M_w = 0.96 \times 10^5$ , 13% DOP,  $\Delta K = 0.5 \text{ MPa}\sqrt{\text{m}}$ .

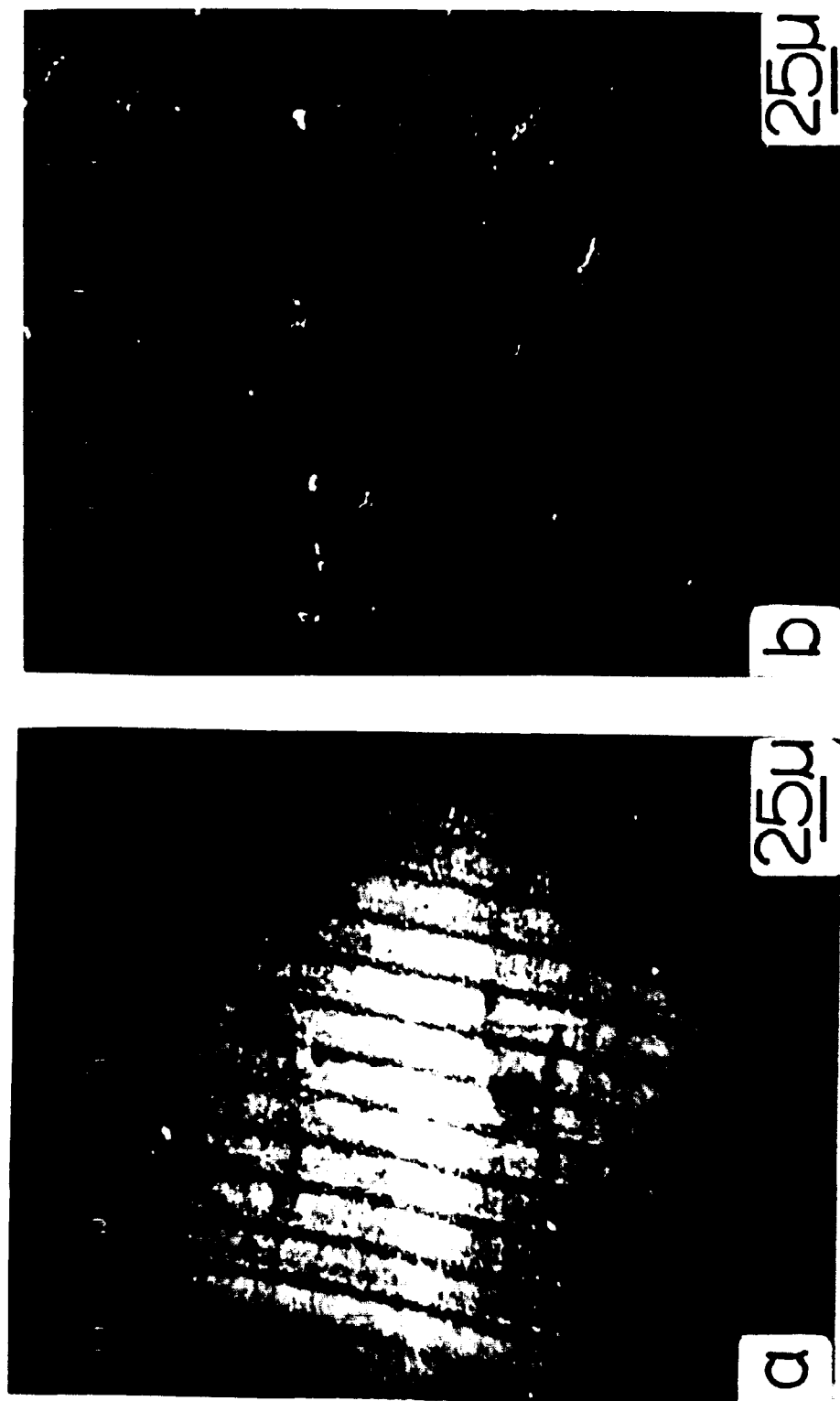


Figure 16. DG band morphology of low M PVC as a function of stress intensity level. (a)  $\Delta K = 0.42 \text{ MPa}\sqrt{\text{m}}$ . (b)  $\Delta K = 0.77 \text{ MPa}\sqrt{\text{m}}$ .  $M_w = 0.97 \times 10^5$ .



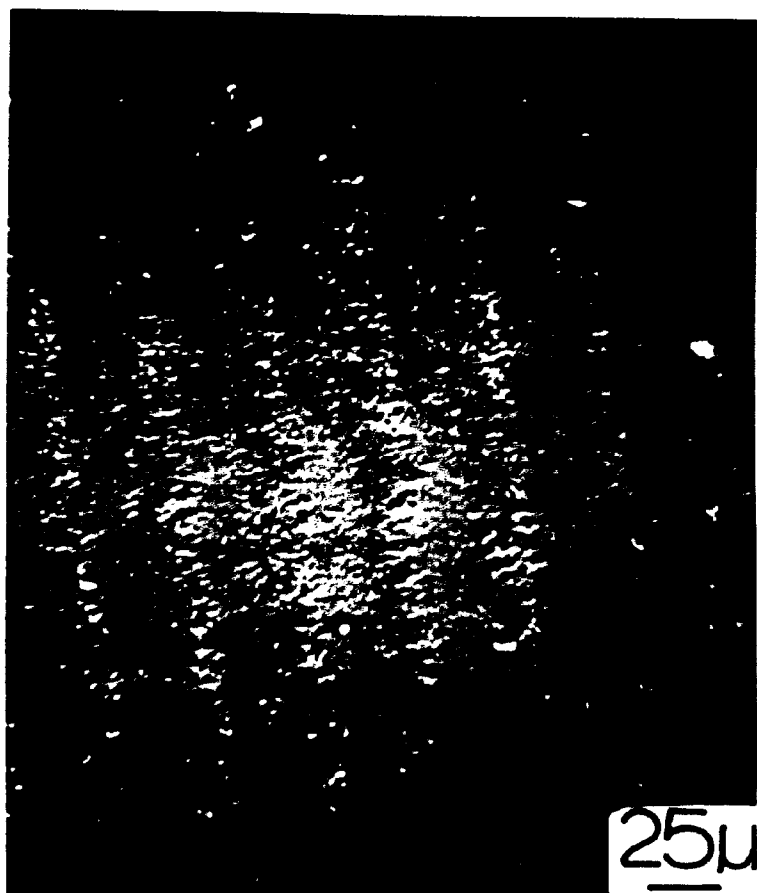


Figure 17. DG band morphology of high M PVC revealing a more ragged structure than at low M.  $M_w = 1.69 \times 10^5$ ,  $\Delta K = 0.66 \text{ MPa}\sqrt{\text{m}}$ .

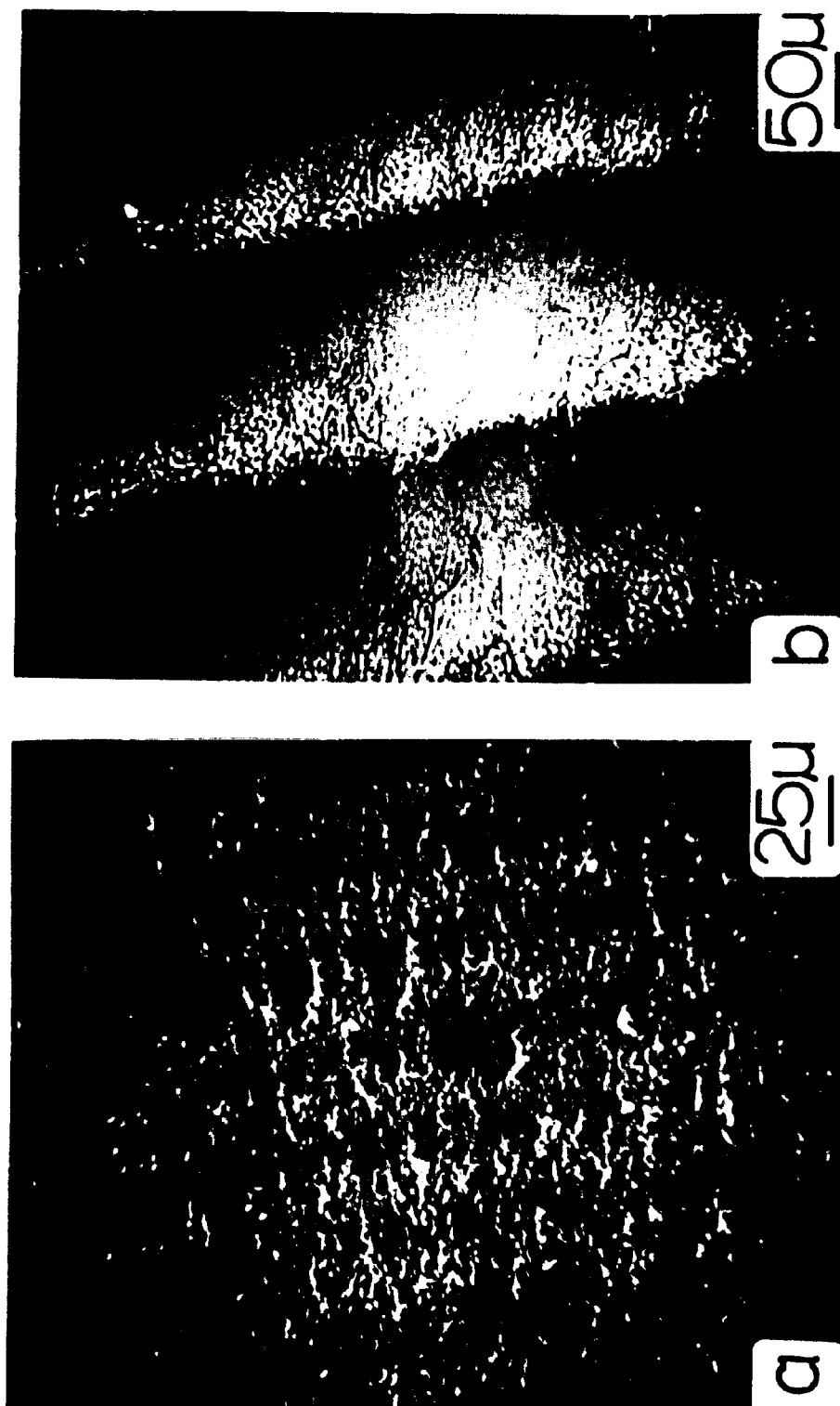


Figure 18. Effect of plasticizer on size and structure of DG band morphology at high  $M$ . (a)  $M_w = 2.1 \times 10^5$ , 0% DOP,  $\Delta K = 0.89 \text{ MPa}\sqrt{\text{m}}$ . (b)  $M_w = 2.25 \times 10^5$ , 13% DOP,  $\Delta K = 0.81 \text{ MPa}\sqrt{\text{m}}$ .

As discussed earlier, an increase in molecular weight serves to enhance craze stability (Figure 12). It is believed that this enhanced craze stability is due to more effective entanglements of the longer molecular chains at high  $M$ ; <sup>(35,36)</sup> thus, craze breakdown is delayed, and void coalescence occurs more slowly. In addition, the enhanced craze stability allows void growth to proceed further prior to instability, resulting in the formation of a more mottled fracture surface.

In the previous section, it was shown that the addition of a plasticizer to the PVC matrix has the effect of decreasing the yield strength, thereby increasing the size of the DG bands. It is also most striking to note that the addition of a plasticizer makes the DG bands more crisp and well-defined. Figures 18a and b show the difference in DG bands at high  $M$  in the unplasticized and plasticized (13% DOP) states, respectively. Notice that there is considerably less tufting on the fracture surface of the plasticized sample compared to that of the unmodified PVC sample. Furthermore, when the plasticizing agent is added, the gradient from large to small voids within the bands becomes regular again.

It is interesting that the CP material supply revealed a more clearly defined set of bands than samples of the same  $M_w$  ( $\sim 1.10 \times 10^5$ ) from series 1 or 2 (see Figure 19a,b). From the previous discussion, this would suggest that the CP material contained a plasticizing component. This conclusion is consistent with the previously observed fact that the inferred  $\sigma_{ys}$  in the CP material was low. In addition, recall that the FCP slope for the

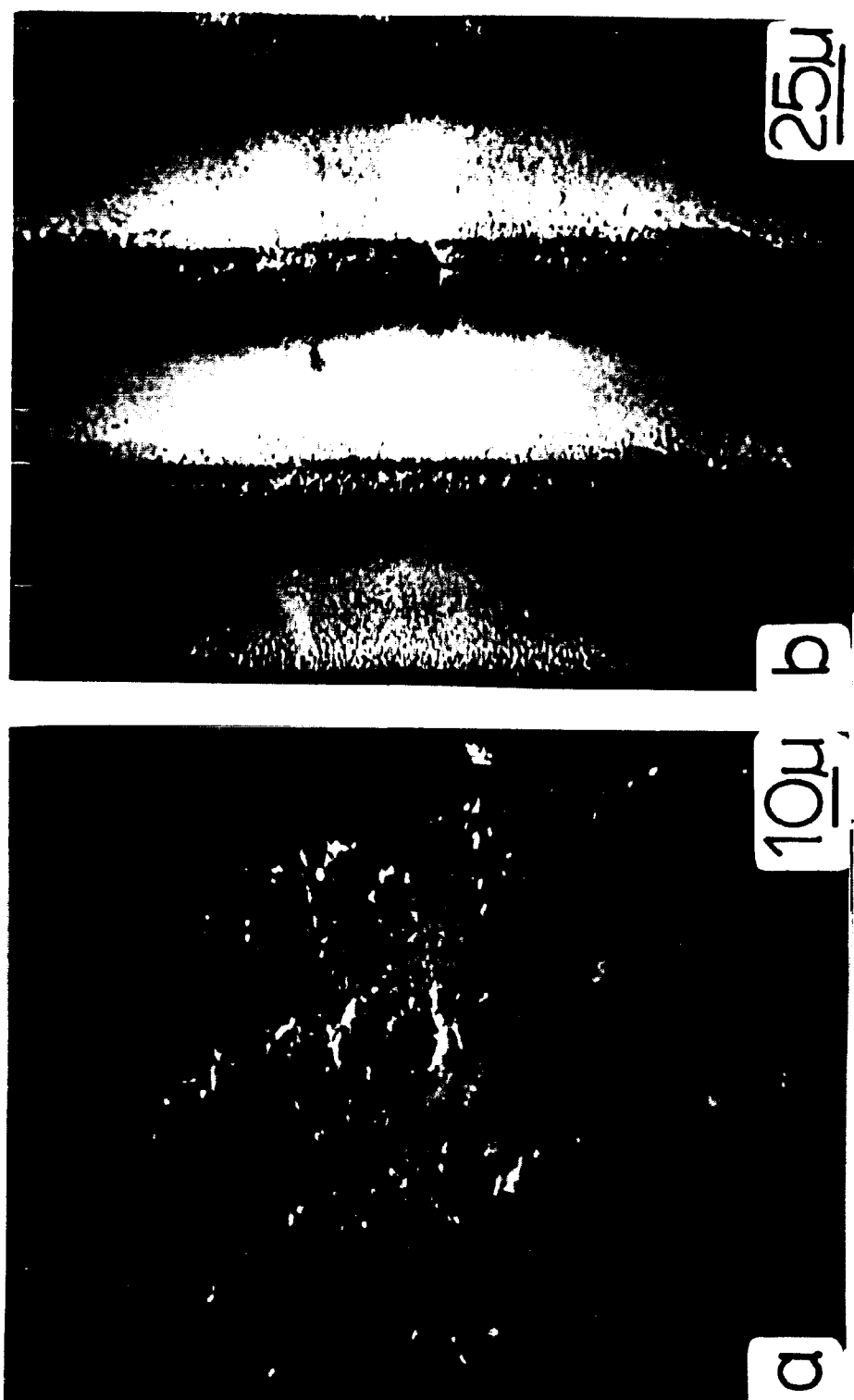


Figure 19. Comparison of DG band morphology of an unmodified PVC fracture sample and a CP PVC fracture sample. (a)  $M_w = 1.06 \times 10^5$ ,  $\Delta K = 0.74 \text{ MPa}\sqrt{\text{m}}$ . (b)  $M_w = 1.07 \times 10^5$ ,  $\Delta K = 0.68 \text{ MPa}\sqrt{\text{m}}$ .

CP material was lower than the FCP slopes of the other molecular weight samples (Figure 3). Finally, characterization of the three PVC supplies showed that the  $T_g$  of the CP material was significantly lower than the respective values for series 1 and 2 (Table 1).

#### PVC micromorphology at low M

Microscopic examination of the fracture surfaces from the lowest M materials (specimens A and 131-1) reveals bands running perpendicular to the direction of crack growth. Measurement of these fracture surface markings in specimens A and 131-1, such as those shown in Figure 20a, indicate that their spacing for the most part is invariant with  $\Delta K$ . This differs from discontinuous growth bands which increase in size as a function of  $\Delta K^2$ . Therefore, it is not clear whether these lines represent specific crack front positions during the test. Further, the micromorphology of these bands do not include the void gradient found to be present on markings known to reflect discontinuous crack extension. As such, determination of  $N^*$  for each of these bands would generate information of questionable significance and for this reason were not included in Figures 12 and 13. These bands are reminiscent of the constant sized-bands found on polystyrene fracture surfaces over a limited  $\Delta K$  range.<sup>(6)</sup> Finally, at stress intensity levels near fast fracture, one finds yet another set of fracture markings in sample A (Figure 20b). The broad light bands represent arrest lines associated with periodic interruptions in the test for the purpose of crack length measurements. The number of narrower lines sandwiched

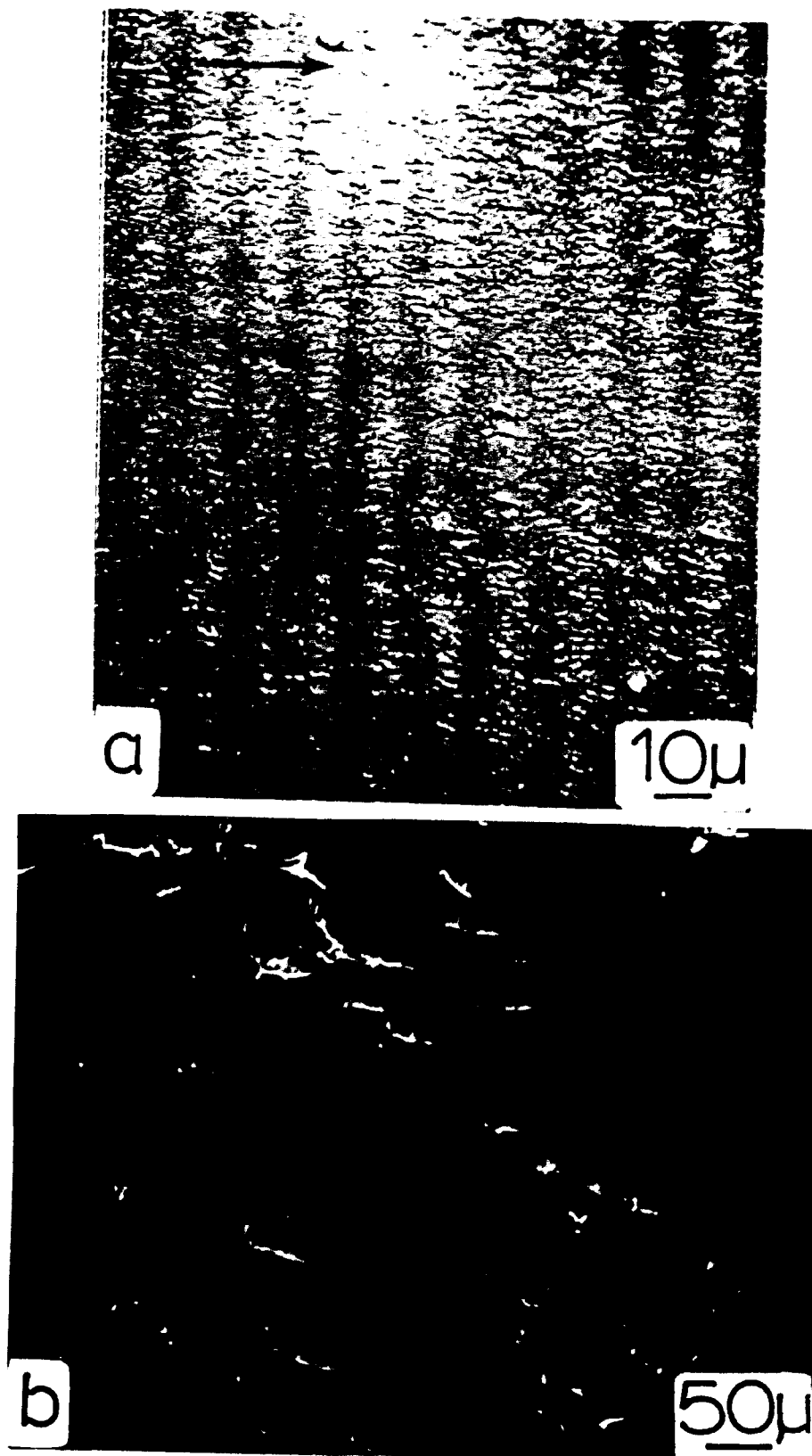


Figure 20. Fracture surface of PVC at very low M. (a) Constant sized bands, found at low  $\Delta K$  levels ( $\Delta K = 0.4 \text{ MPa}\sqrt{\text{m}}$ ). (b) Striation-like lineage (within crack arrest marks) corresponding to macroscopic growth rate, near fast fracture.  $\Delta K = 0.64 \text{ MPa}\sqrt{\text{m}}$ .

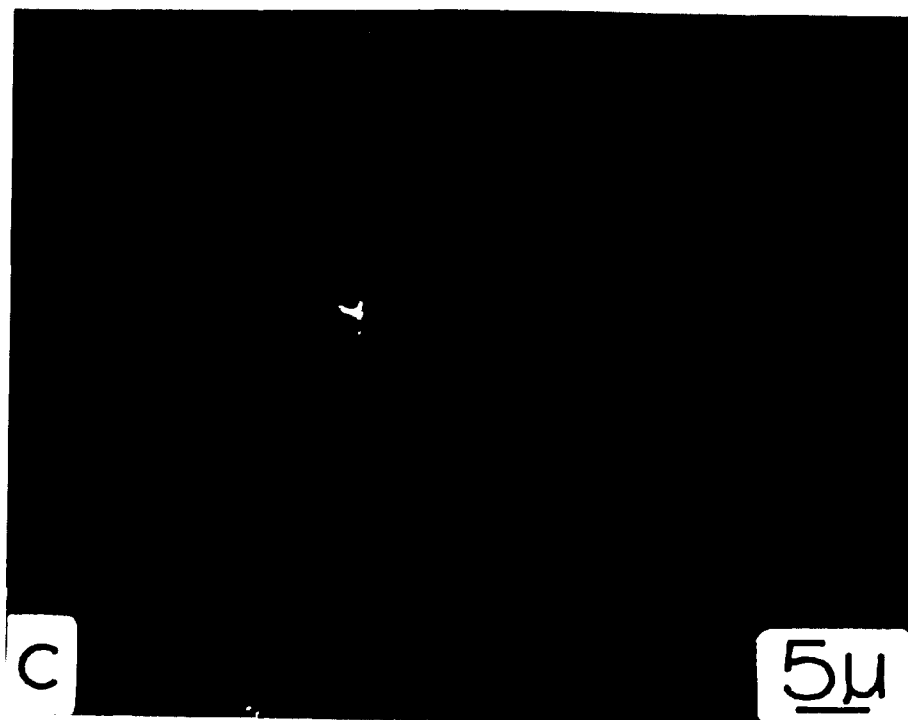


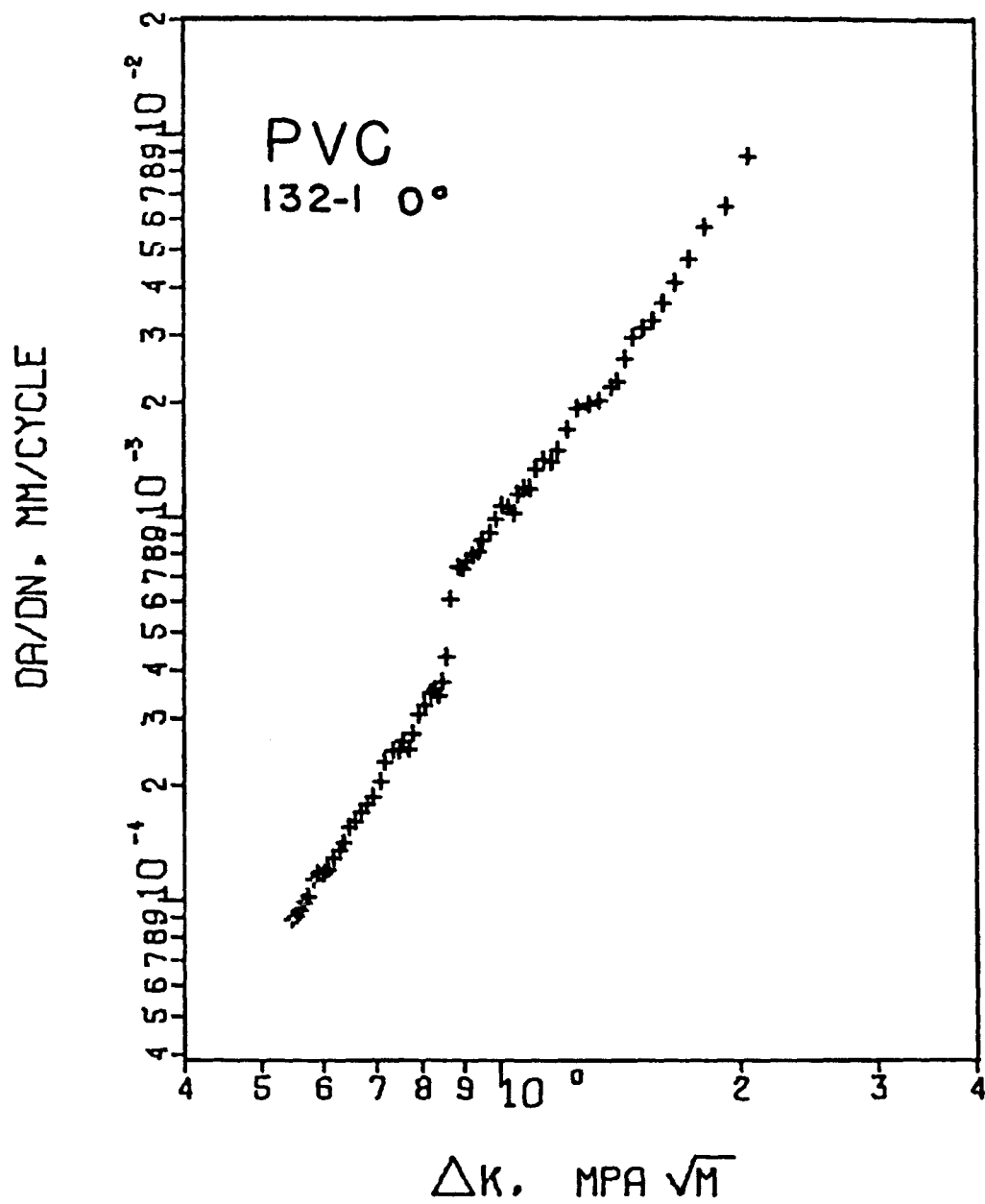
Figure 20. (c) High magnification of bands in (b), revealing finer internal lineage. Markers indicate boundaries of each "striation".  $M_w = 0.61 - 0.67 \times 10^5$ .

between these arrest bands corresponds to the number of loading cycles between successive crack length readings and implies that these markings are striations. And yet, these "striations" are themselves composed of an integral number of narrower lines similar to those found at low  $\Delta K$  levels (Figure 20c). A striation substructure of this type is not known to correspond to any specific cyclic loading event, such as a part of the loading cycle. Consequently, these additional fracture lines are believed to be caused by plastic flow-induced perturbations of an already formed fatigue fracture surface. Similar ripple-type markings have been shown to exist in metals.<sup>(37)</sup>

Sample 132-1 ( $M_w = 0.95 \times 10^5$ ) was found to exhibit a change in fatigue crack growth mechanism midway through the fatigue test. This transition is associated with the discontinuity in crack growth rate at a  $\Delta K$  of 0.8 to 1.0 MPa $\sqrt{m}$  (Figure 21). Furthermore, the slope of the  $da/dN - \Delta K$  plot after the transition decreased from 3.25 to 2.75. This transition occurred in both the 0° and 90° test orientations at approximately the same stress intensity level. At low  $\Delta K$  values, the fracture surface was yellowish in color but then changed sharply at the transition to a multicolor rainbow pattern. This observation is similar to the transition noted in polystyrene, where the multicolor appearance was found to be due to the early stages of crack growth through craze bundles.<sup>(6)</sup>

Prior to the transition, cracking occurred by discontinuous growth, as observed in the higher molecular weight samples. When viewed under the light microscope, these bands revealed a rough





texture due to the void gradient and stretch zone which make up each band. Beyond the transition, the bands appeared as undulations on the fracture surface and were composed of small, regular sized voids, thereby, giving them a smoother texture (Figure 22a). With increasing  $\Delta K$ , these new bands increased in size and were found to be close to, but smaller than predicted DG band widths. At still higher  $\Delta K$  levels, these bands were seen to contain a periodic array of finer fracture lines which changed in spacing across the dimension corresponding to the larger band widths (Figure 22b). Just short of fast fracture, the distance between these fine lines was found to correspond to the macroscopic growth rate; at the same time, the larger undulations were no longer identifiable. Similar fatigue behavior has been noted by Mackay, et al.<sup>(38)</sup> for the case of fatigue in polycarbonate. Further studies are needed to provide explanations for the transition in fatigue crack growth mechanisms in these two materials.

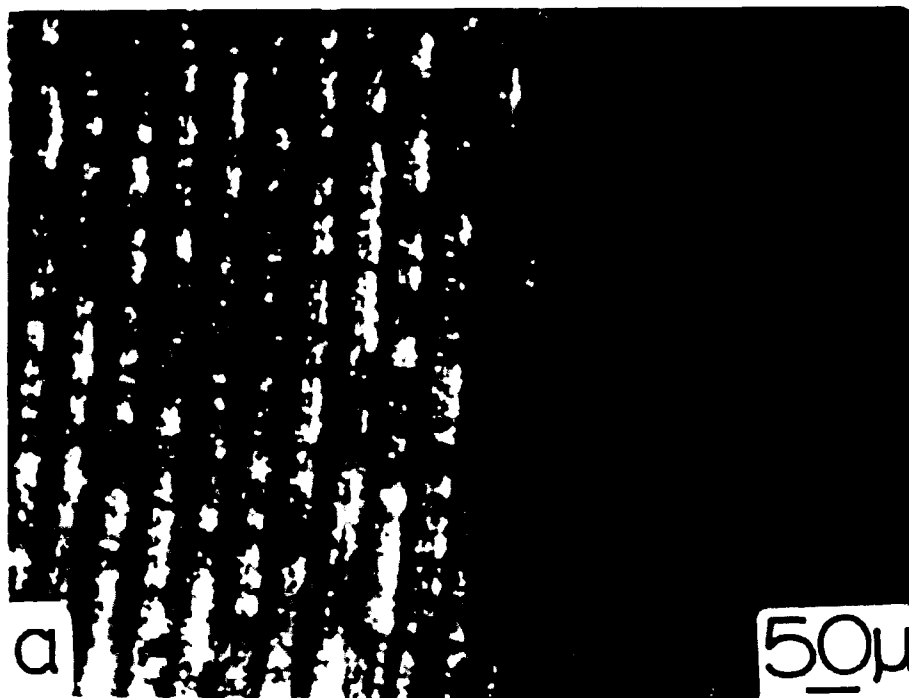


Figure 22. (a) Light micrograph of fracture transition of sample 132-1. Light patchy areas indicate roughness of DG bands, while lower contrast region indicates smoother textured.  $\Delta K = 0.8 \text{ MPa}\sqrt{\text{m}}$ .

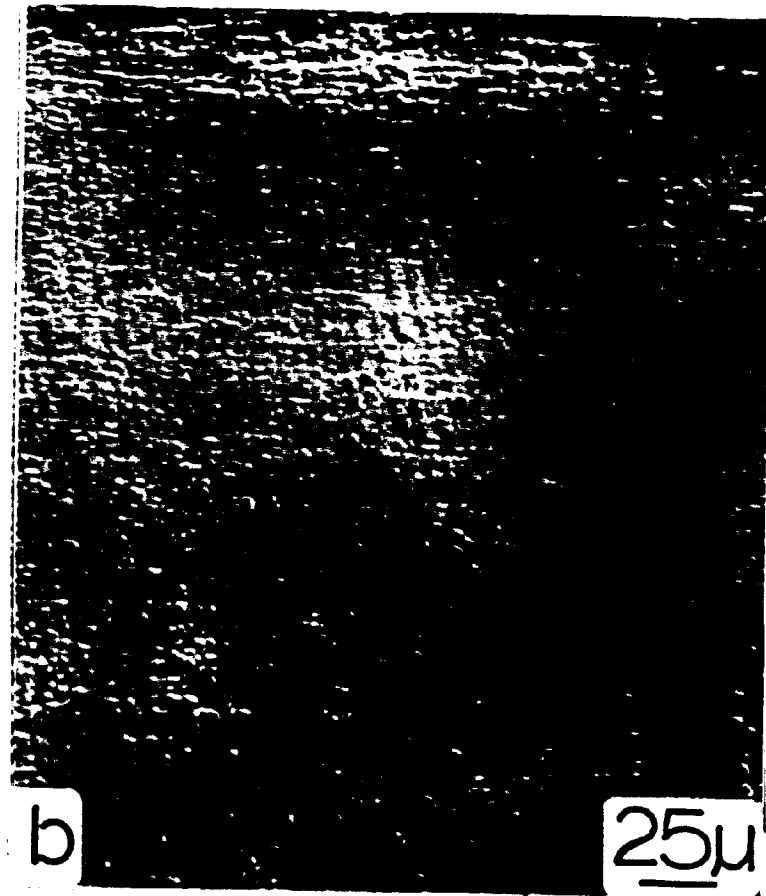


Figure 22. (b) Periodic array of finer fracture lines comprising each larger band. Marks indicate boundaries of large bands.  $\Delta K = 1.76 \text{ MPa}\sqrt{\text{m}}$ .  $M_w = 0.95 \times 10^5$ .

### Conclusions

Over the molecular weight range studied, M is found to strongly affect the fatigue crack propagation resistance of PVC. Increasing M initially results in a sharp decrease in the fatigue crack growth rate  $da/dN$ , with the decline approaching a limiting value at high M. Residual orientation due to compression molding or extrusion of PVC does not markedly affect FCP resistance; however, at low molecular weights fatigue crack growth resistance is slightly enhanced when the test load axis is  $0^\circ$  to the direction of residual chain alignment.

Discontinuous crack growth is found to be the major fatigue cracking mechanism in PVC. The inferred yield strength is not strongly dependent on M or test orientation, but does vary markedly with plasticizer content. Craze stability, i.e., the number of loading cycles required to strike through a craze, is found to be strongly dependent on molecular weight. Plasticizer additions also contribute toward an improvement in discontinuous growth band stability, though to a lesser degree.

While DG band size is not dependent on M, the micromorphology of the discontinuous growth band varies strongly with molecular weight. With increasing M, the DG bands become less clean; both the void gradient and stretch zone lose their distinctiveness and the boundaries between the bands become difficult to identify. Finally, the crisp internal structure of the DG bands found at low M is restored to that observed in the high M samples through the addition of a plasticizing agent.

## References

1. Hutchinson, S. J. and Benham, P. P., Plast. Polym., Vol. 102, April, 1970.
2. Manson, J. A. and Hertzberg, R. W., CRC Crit. Rev. Macromol. Sci., Vol. 1, 1973, p. 433.
3. Hertzberg, R. W. and Manson, J. A., Fatigue of Engineering Plastics, Academic Press, New York, in press.
4. Schultz, J. M., in "Treatise on Materials Science and Technology," Vol. 10B, M. M. Schultz, Ed., Academic Press, New York, 1977.
5. Paris, P. C., "Fatigue - An Interdisciplinary Approach," Syracuse University Press, Syracuse, 1964, p. 107.
6. Skibo, M. D., Hertzberg, R. W. and Manson, J. A., J. Mater. Sci., Vol. 11, 1976, pp. 479-490.
7. Skibo, M. D., Hertzberg, R. W., Manson, J. A. and Kim, S. L., J. Mater. Sci., Vol. 12, 1977, pp. 531-542.
8. Hertzberg, R. W., Skibo, M. D. and Manson, J. A., ASTM STP 675, 1979, p. 471.
9. Elinck, J. P., Bauwens, J. C. and Homes, G., Int. J. Fract. Mech., Vol. 7, No. 3, 1971, p. 277.
10. Bretz, P. E., unpublished research.
11. Hertzberg, R. W., Skibo, M. D. and Manson, J. A., J. Mater. Sci., Vol. 13, 1978, p. 1038.
12. Dugdale, D. S., J. Mech. Phys. Solids, Vol. 8, 1960, p. 100.
13. Skibo, M., Manson, J. A. and Hertzberg, R. W., J. Macromol. Sci.-Phys., Vol. B14, No. 4, 1977, pp. 525-543.

14. Skibo, M. D., Manson, J. A., Webler, S. M., Hertzberg, R. W. and Collins, E. A., in Durability of Macromolecular Materials, R. K. Eby, Ed., ACS, Washington, D. C., 1979, p. 311.
15. Kim, S. L., Skibo, M., Manson, J. A. and Hertzberg, R. W., Polym. Eng. Sci., Vol. 17, No. 3, March 1977, p. 194.
16. Kim S. L., Janiszewski, J., Skibo, M. D., Manson, J. A. and Hertzberg, R. W., Polym, Eng. Sci., Vol. 19, No. 2, 1979, p. 145.
17. Manson, J. A., Hertzberg, R. W., Kim, S. L. and Wu, W. C., in Toughness and Brittleness of Plastics, R. D. Deanin and A. M. Crugnola, Eds., ACS, Washington, D. C., 1976, p. 146.
18. Hertzberg, R. W., Manson, J. A. and Skibo, M., Polym.Eng. Sci., Vol. 15, No. 4, April 1975, p. 252
19. Skibo, M. D., Hertzberg, R. W. and Manson, J. A., Int. Conf. of Fracture, Waterloo, Canada, Vol. 3, June 1977, p. 1127.
20. Hertzberg, R. W., Manson, J. A. and Skibo, M. D., Polymer, Vol. 19, March 1978, p. 358.
21. Martin, G. C. and Gerberich, W. W., J. Mater. Sci., Vol. 11, 1976, pp. 231-238.
22. Wann, R. J., Martin, G. C. and Gerberich, W. W., Polym. Engr. Sci., Vol. 16, No. 9, 1976, p. 645.
23. Skibo, M. D., "The Effect of Frequency, Temperature, and Materials Structure on Fatigue Crack Propagation in Polymers," Ph.D. Dissertation, Lehigh University, 1977.
24. Janiszewski, J., Hertzberg, R. W. and Manson, J. A., to be presented, 13th Natl. Symp. on Frac. Mech., June 1980.

25. ASTM Standard E647-78T, Annual Book of ASTM Standards, 1979.
26. Gotham, K. V. and Scrutton, I. N., Polymer, Vol. 19, No. 3, 1978, p. 341.
27. Clark, W. G., Jr. and Hudak, S. J., Jr., J. of Testing and Eval., Vol. 3, No. 6, 1975, p. 454.
28. Mills, N. J., Engr. Frac. Mech., Vol. 6, 1974, p. 537.
29. Bauwens, J. C., Bauwens-Crowet, C. and Homes, G., J. Polym. Sci., Part A-2, Vol. 7, 1969, p. 1745.
30. Cross, A., Haward, R. N. and Mills, N. J., Polymer, Vol. 20, March 1979, p. 288.
31. Pezzin, G., Ajroldi, G., Casiraghi, T., Garbuglio, C. and Vittadini, G., J. Appl. Poly. Sci., Vol. 14, 1972, p. 1839.
32. Rimnac, C. M. and Webler, S. M., unpublished research.
33. Martin, J. R., Johnson, J. F. and Cooper, A. R., J. Macromol. Sci-Revs. Macromol. Chem., Vol. 68, No. 1, 1972, pp. 57-199.
34. Haward, R. N., The Physics of Glassy Polymers, Wiley, New York, 1973.
35. Fellers, J. F. and Kee, B. F., J. Appl. Polym. Sci., Vol. 18, 1974, p. 2355.
36. Wellenhoff, S. and Baer, E., J. Macromol. Sci.-Phys., Vol. B11, 1976, p. 367.
37. Beachem, C. D. and Meyn, D. A., Illustrated Glossary of Fractographic Terms, Sect. 2, NRL Memorandum Report 1547, Washington, D. C., 1964.
38. Mackay, M. E., Teng, T.-G. and Schultz, J. M., J. Mater. Sci., Vol. 14, 1979, pp. 221-227.



### Vita

Clare Marie Rimnac was born February 2, 1956, in Chicago, Illinois, to George C. and Paula (O'Gorman) Rimnac. She received her elementary education in the Glenview School District, Glenview, Illinois and graduated from Maine Township High School North, Des Plaines, Illinois in 1974.

In May 1978, Ms. Rimnac graduated from Carnegie-Mellon University with the degree of Bachelor of Science in Metallurgy and Materials Science. While at Carnegie-Mellon she was mentioned on the Dean's list and was President of the Student Metallurgical Society.

Since August 1978, Ms. Rimnac has been a Research Assistant in the Department of Metallurgy and Materials Engineering at Lehigh University. She will continue as Research Assistant and Instructor while pursuing her doctorate.